

# A COMPARISON OF VARIOUS STRESS RUPTURE LIFE MODELS FOR ORBITER COMPOSITE PRESSURE VESSELS AND CONFIDENCE INTERVALS

Lorie Grimes-Ledesma  
Jet Propulsion Laboratory, California Institute of Technology

Pappu L.N. Murthy  
NASA Glenn Research Center

S. Leigh Phoenix  
Cornell University

Ronald Glaser  
Lawrence Livermore National Laboratory, University of California

In conjunction with a recent NASA Engineering and Safety Center (NESC) investigation of flight worthiness of Kevlar Overwrapped Composite Pressure Vessels (COPVs) on board the Orbiter, two stress rupture life prediction models were proposed independently by Phoenix and by Glaser. In this paper, the use of these models to determine the system reliability of 24 COPVs currently in service on board the Orbiter is discussed. The models are briefly described, compared to each other, and model parameters and parameter error are also reviewed to understand confidence in reliability estimation as well as the sensitivities of these parameters in influencing overall predicted reliability levels.

Differences and similarities in the various models will be compared via stress rupture reliability curves (stress ratio vs. lifetime plots). Also outlined will be the differences in the underlying model premises, and predictive outcomes. Sources of error and sensitivities in the models will be examined and discussed based on sensitivity analysis and confidence interval determination. Confidence interval results and their implications will be discussed for the models by Phoenix and Glaser.

## **Stress Rupture as an Aging Orbiter Concern**

Composite Overwrapped Pressure Vessels (COPVs) consist of a thin metallic liner overwrapped with a high strength filament wound composite. Because the composite carries the majority of the pressure load during operation, the amount of higher weight metallic structure needed is reduced. This results in a significantly lower mass pressure vessel as compared to an all-metallic vessel. The overall savings achieved based on the required 24 COPVs per Orbiter, was 700 lb. over monolithic titanium tanks.<sup>1</sup> On the Orbiter; these vessels are used for storing pressurant inert gases for propulsion systems (OMS- Orbital Maneuvering System, RCS- Reaction Control System, MPS- Main Propulsion System) and environmental systems (ECLSS- Environmental Control System). Locations of these COPVs on board the Orbiter are shown in Figure 1.

COPVs are susceptible to many of the same failure modes as metallic pressure vessels, but additional considerations are required to ensure that the vessel has a reliable composite overwrap. The majority of these composite failure modes were adequately mitigated during the design of the vessels, but a re-assessment of the stress rupture failure mode was necessary for the Orbiter COPVs because most of the COPVs had been in service since the beginning of the Shuttle program in the early 1980's.<sup>1</sup>

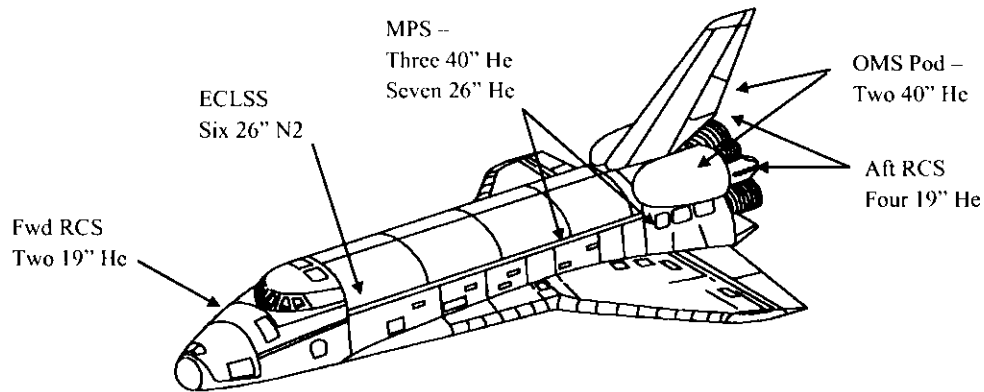


**Figure 1. Orbiter COPV locations.**

Stress rupture is the failure of a fiber as a function of sustained load and time. It is understood mainly on a phenomenological level and stress rupture life prediction methodologies are based on stochastic modeling. The following have been repeatedly observed by many researchers.<sup>2-7</sup>

1. Stress rupture lifetime is mainly a function of composite fiber stress (usually expressed as a percentage of short-term strength, called the stress ratio).
2. Stress rupture is a material property of the fiber although matrix properties play a role in terms of influencing the mechanics of inter-fiber load sharing prior to catastrophic failure. Different fiber types (carbon, Kevlar, glass) have different stress rupture characteristics.
3. Stress rupture life data can be fit using Weibull statistics with a distribution function of the form:

$$P(s) = 1 - e^{-\left(\frac{x}{\alpha}\right)^\beta} \quad (1)$$

where  $x$  is stress,  $\alpha$  is the scale parameter and  $\beta$  is the shape parameter.

4. During room temperature testing, slow degradation of the fiber with time is not observed, i.e. the fiber appears to maintain its original strength until it suddenly fails, and thus, strength (burst) testing of aged composites cannot provide an indication of remaining stress rupture life (for tests at elevated temperatures, however, a reduction in burst strength has been observed for Kevlar).

Stress rupture of a composite is due to the failure of the fiber. At present, no single mechanism has been proven definitively as the leading cause for failure in Kevlar or carbon, although for glass, a water-based stress-corrosion mechanism has been demonstrated.<sup>8</sup> For Kevlar, chain scission/slippage models and time-dependent continuum crack growth models have been suggested, but the parameters in the end must be established empirically.<sup>9, 10</sup> Ties between fiber stress rupture failure and the overall failure of the composite have been analytically studied. A progressive failure model has been developed by Phoenix, and others at Cornell, based on a progression beginning with chain scission/slippage within the fiber prior to the failure of adjacent fibers and shear failure of the resin leading to fiber break cluster growth and failure of the composite.<sup>9</sup> Since load transfer to other fibers occurs through shear transfer in the resin during the failure of a composite, the resin does have an effect on the stress rupture life, but the effect is

not first order for Kevlar fiber at typical operating stress levels. Matrix effects are more significant in the case of carbon fibers.<sup>11</sup>

Stress rupture life testing for Kevlar has been performed primarily by Lawrence Livermore National Laboratory (LLNL) and Cornell University with Kevlar material characterization contributions from the Y12 Plant at Oak Ridge National Laboratory and Sandia National Laboratories. These tests have consisted of single-fiber, fiber-bundle, resin impregnated strand (or tow tests), and COPV testing at a single constant stress level.<sup>12-15</sup> Although most of this testing has been conducted at ambient temperature, temperature acceleration has been performed to decrease the stress rupture life based on the concept that scission rate increases with temperature. Testing of this idea was performed at LLNL and Cornell.<sup>16</sup>

Although models based on data from LLNL, Cornell, and DOE are available in the literature, they are not directly comparable to any other COPV design as published. For the purposes of evaluation of the Orbiter COPVs, the pressure vessel data developed at LLNL were used because this data most closely resembles the structure of the Orbiter COPVs. However, modifications to the data as published were required. Changes were made to account for the pressure carrying effects of the liner, the effects of strength variations between different spools used to overwrap the COPVs, and compensation for differences in ultimate burst strength of the composite due to differences in pressurization rate between the Orbiter COPVs and LLNL test COPVs.

The establishment of a relationship between the very-different designs of the LLNL test COPVs and the Orbiter vessels was non-trivial and was a major thrust of the study. The development of relationships between burst strength, composite operational stress level, and fiber quantity were necessary. Detailed discussion of these relationships will be reported elsewhere.

To determine the continued flightworthiness of Orbiter COPVs, the NESC sponsored a study of forecasts based on independently derived models for stress rupture. Since Leigh Phoenix at Cornell University, Ron Glaser at Lawrence Livermore National Laboratory (LLNL), and Ernest Robinson at the Aerospace Corporation had already established independent frameworks for the modeling of stress rupture of Kevlar as evidenced in academic literature over the past 30 years or so, they were chosen to provide stress rupture life models to the NESC for the Orbiter COPVs. The Phoenix and Glaser models will be discussed and compared in this paper although the model of Robinson has equal merit and will be discussed in detail in a future publication.

### Phoenix Model

The Phoenix model has been developed over the past 27 years and is well documented in the literature. It is based on a Weibull distribution framework for strength and lifetime with the embodiment of a power law to describe damage in a composite versus stress level. Derivation of the model is available in references 9 and 17, where the power-law in stress level (with temperature dependence) is derived from thermally activated chain scission using a Morse potential as a model. While the basic concepts for the model are the same as those previously developed, the parameters are based on an entirely new analysis of the LLNL pressure vessel data. Though not discussed here, the model has also been applied to strand data as well, with comparable results. In the simplest setting of constant stress applied quickly and maintained over a long time period, the basic equation for the model is below.

$$P(t, \sigma) = 1 - \exp \left[ - \left\{ \left( \frac{t}{t_{cref}} \right) \left( \frac{\sigma_{op}}{\sigma_{burst}} \right)^n \right\}^\beta \right] \quad (2)$$

The ratio of  $\sigma_{op}/\sigma_{burst}$  is the ratio of fiber stress at operating pressure to fiber stress at burst pressure (stress ratio),  $t$  is time,  $t_{c,ref}$  is a reference time,  $\rho$  is the power law exponent, and  $\beta$  is the Weibull shape parameter for lifetime. The value for  $\sigma_{burst}$  accounts for pressurization rate differences between Orbiter COPVs and the LLNL test COPVs. This strain rate effect has been discussed in reference 4 and will be discussed in later publications in more detail. The strain rate difference between Orbiter COPVs and LLNL test COPVs is inherent in the Phoenix model because the stress ratios for the LLNL vessel data have been modified to account for this rate. The model is shown for a single stress level over time, but for more general time histories a memory integral is used to accumulate damage (similar to Miner's rule for fatigue) at different stress levels. Also, at very high stress levels a second quantity within square brackets and of similar structure to the first must also be included with a leading minus sign as well (i.e., in a weakest damage mechanism framework). This second quantity has different parameter values, especially a much higher  $\rho$  value.

In the Phoenix model, values for the parameters  $t_{c,ref}$ ,  $\rho$ , and  $\beta$  are determined based on the LLNL vessel data and are influenced by observations of stress rupture behavior of strands and single fibers. Values for these parameters determined by Phoenix for the LLNL vessel data are shown in Table 1. The power law exponent,  $\rho$ , is the inverse of the slope of the logs of the scale parameter of the stress rupture data and the stress ratio. The parameter  $t_{c,ref}$  is an anchor point determined from this slope and an instantaneous reference strength. In the Phoenix model, both  $\rho$  and  $\beta$  are based primarily on the LLNL vessel data but were chosen such that all data available (which includes data from other Kevlar COPVs and strands) are considered. In this way the parameters are determined from broader observations of stress rupture data as a whole, making the resulting reliability estimations consistent with all stress rupture data. This "big picture" approach is a unique feature of the Phoenix model.

**Table 1. Parameter values for the Phoenix model.**

Parameter	Value
$\rho$	24
$\beta$	1.2
$t_{c,ref}$	0.5456

Based on the Phoenix model, a series of reliability quantile curves can be developed for use in design that allow estimation of the lifetime for a chosen quantile. Figure 2 shows the stress rupture curve for the Phoenix model. This approach can be used by choosing an appropriate combination of stress ratio and lifetime to ensure a desired reliability during the design of a COPV. Analysis based on this approach is employed currently by COPV manufacturers.

However, in the case of the Orbiter, the COPVs had been successfully operated for a long period of time already, so a conditional probability approach was used (in essence ruling out unusually short lived vessels within the population since none actually occurred). In this approach, a reference time is chosen and all successful history prior to the reference is considered in the analysis. In the case of the Orbiter vessels, the reference time was chosen as return-to-flight. Because the vessels had successfully "survived" up to the reference time this successful past history is credited in the analysis. The conditional reliability equation for the Phoenix model is below.

$$F(t, \sigma) = 1 - \exp \left[ - \left\{ \left( \frac{t_1}{t_{cref}} \right) \left( \frac{\sigma_{op1}}{\sigma_{ref}} \right)^\rho + \frac{\Delta t}{t_{cref}} \left( \frac{\sigma_{op2}}{\sigma_{ref}} \right)^\rho \right\}^\beta + \left( \frac{t_1}{t_{cref}} \left( \frac{\sigma_{op1}}{\sigma_{ref}} \right)^\rho \right)^\beta \right] \quad (3)$$

In this equation, two new terms appear, one for a second stress level and another to account for past history. This conditional reliability equation was used in all Phoenix calculations for Orbiter reliability estimates for future flights.

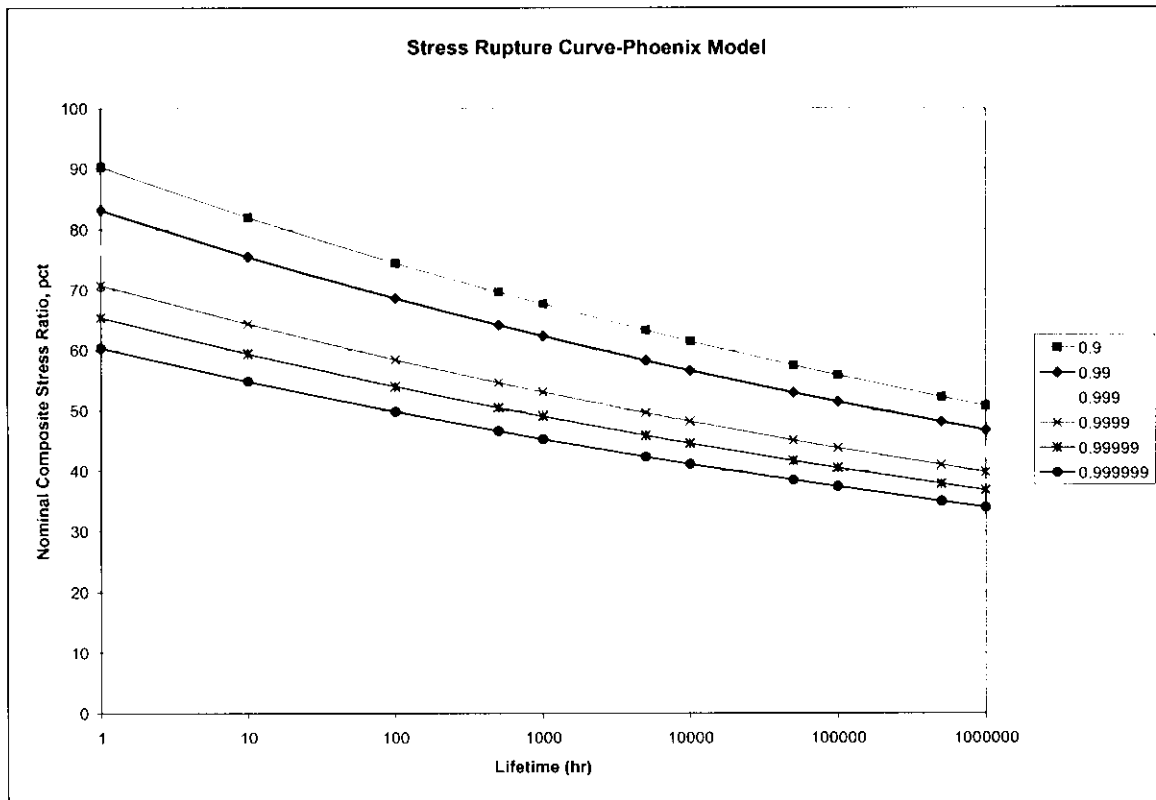


Figure 2. Phoenix Stress Rupture Curve. Quantiles are for probability of survival.

### Glaser Model

The Glaser model was developed independently of the Phoenix model during the same time frame and is also based on a Weibull distribution with a generalized power law. The equation for the survival probability in the Glaser model is below.

$$P\{T_s > t\} = \exp\left[-\left(\frac{t}{a(s)}\right)^{b(s)}\right] \quad (4)$$

where

$$\alpha(s) = \log a(s) = \beta_1 + \beta_2 \log s$$

$$\sigma(s) = 1/b(s) = \beta_3$$

The model simplifies to:

$$P\{T_s > t\} = \exp\left[-\left(\frac{t}{e^{\beta_1} s^{\beta_2}}\right)^{1/\beta_3}\right] \quad (5)$$

In the Glaser model,  $s$  is the stress ratio, and the  $\beta$ 's are coefficients based on the LLNL vessel data. Unlike the Phoenix model, no strain rate adjustments were applied to the LLNL vessel burst strengths to account for strain rate differences relative to the LLNL vessels.

In the model, the  $\beta$  values are determined based on a maximum likelihood methodology developed by Glaser and are shown for the LLNL COPV data in Table 2.

**Table 2. Coefficient values for the Glaser model.**

Parameter	Value
$\beta_1$	109.4367
$\beta_2$	-23.602
$\beta_3$	0.8088

While the form of the Glaser model is similar to that presented in the literature and in LLNL reports<sup>2,14</sup>, estimation of  $\alpha(s)$  and  $\sigma(s)$  was changed to allow a comparison with the Orbiter COPVs. The original forms had a stress varying shape parameter -  $b(s)$ , which was a polynomial function of stress ratio, rather than a constant. The model was changed to a constant shape parameter to focus the model in the center of the data to minimize the effect of the data at lower and upper tails of the distribution and extremes of stress ratio.

As discussed previously, the model can be represented graphically in a set of stress rupture curves. Glaser was the originator of this representational method and curves based on his model are shown in figure 3. While these curves are applicable to the Orbiter COPVs, curves based on previous versions of the Glaser model are not directly applicable to the Orbiter COPVs.

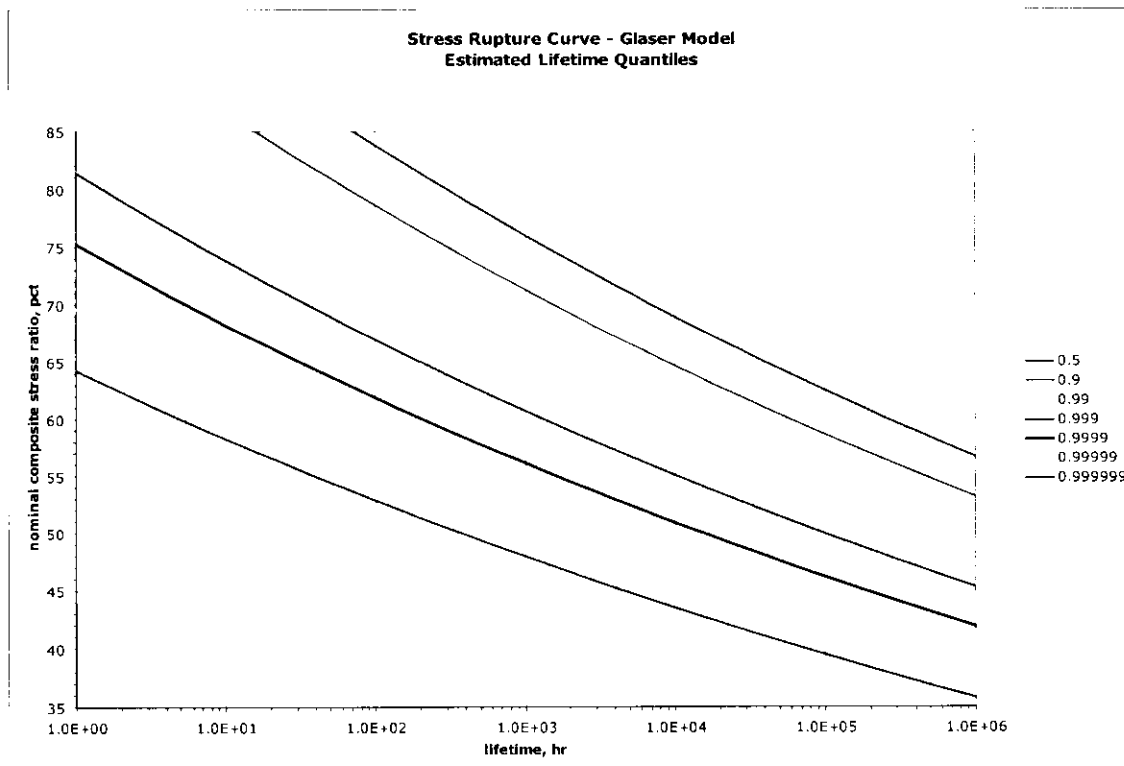


**Figure 3. Glaser Stress Rupture Curve. Quantiles are for probability of survival.**

Although these stress rupture curves provide an expedient method of determining reliability during design, Glaser also chose a conditional reliability approach for the Orbiter COPVs. The conditional reliability version of the Glaser model is below.

$$M(s,t,s^*,\Delta) = 1 - P\{T_{s^*} > t^* + \Delta | T_{s^*} > t^*\} = 1 - \exp\left[-\left(\frac{t^* + \Delta}{e^{\beta_1} s^* \beta_2}\right)^{1/\beta_3} + \left(\frac{t^*}{e^{\beta_1} s^* \beta_2}\right)^{1/\beta_3}\right] \quad (6)$$

In this formula, another term is created to account for the successful past history of the Orbiter COPVs. This conditional reliability equation was used in all Glaser calculations for Orbiter reliability estimates for future flights.

### Comparison of Reliability Models from Glaser and Phoenix

Both the Phoenix and Glaser models are based on a power-law framework within the Weibull distribution. This methodology has a basis in early composites failure theory developed by Coleman.<sup>18</sup> The models provide virtually indistinguishable reliability estimates for the Orbiter COPVs, especially when conditional reliability is used. A comparison between results for each model is shown in table 3.

**Table 3. Comparison of Reliability Estimates for Using Phoenix and Glaser Models. Estimates are calculated for the next scheduled flight.**

Vessel Type	Stress Ratio for Phoenix Model	Stress Ratio for Glaser Model	Past Accumulated Hours	Hours for One Future Mission	No. of Vessels	Non-Conditional		Conditional	
						Phoenix	Glaser	Phoenix	Glaser
OMS	0.575	0.604	4151	252	1	0.994571361	0.995182204	0.99960116	0.99899579
OMS	0.575	0.604	3983	252	1	0.994833253	0.99542157	0.99960434	0.99899579
RCS	0.515	0.541	7551	630	2	0.999066453	0.999187175	0.99990573	0.99962693
RCS	0.515	0.541	6620	395	2	0.999202759	0.999309176	0.99994256	0.99976608
RCS	0.515	0.541	6112	249	2	0.999275571	0.999374093	0.99996443	0.99985253
MPS he	0.54	0.576	858	24	3	0.999596528	0.999483792	0.99998642	0.99990638
MPS He	0.47	0.494	858	24	7	0.999982728	0.999986366	0.99999942	0.99999418
ECLSS N2-1	0.445	0.468	74495	648	1	0.999891619	0.999899715	0.99999887	0.99999373
ECLSS N2-2	0.445	0.468	74495	648	1	0.999891619	0.999899715	0.99999887	0.99999373
ECLSS N2-3	0.445	0.468	74408	648	1	0.999891771	0.999899859	0.99999887	0.99999373
ECLSS N2-4	0.445	0.468	65910	648	1	0.999906428	0.999913803	0.99999889	0.99999373
ECLSS N2-5	0.445	0.468	61793	648	1	0.999913397	0.999920409	0.99999891	0.99999373
ECLSS N2-6	0.445	0.468	22548	648	1	0.999974169	0.999977116	0.99999911	0.99999373
<b>Reliability for Entire System of COPVs=</b>						<b>0.986066333</b>	<b>0.987510562</b>	<b>0.99899791</b>	<b>0.99710314</b>

Table 3 shows the probability of survival estimates using the basic models (non-conditional) and conditional reliability models. For each of the vessel types, the reliability is determined as a function of the number of vessels in that type, so it's the single vessel reliability to the number of vessels of that type. To determine the overall system level reliability, the reliabilities of each vessel type are multiplied to arrive at a reliability estimate for the Orbiter system of COPVs. This similarity of the results despite their independent development lends credibility to both models.

A more general comparison of the basic models is observed in stress rupture curve comparisons. Figure 4 shows a stress rupture curve for the 0.999 and 0.99999 quantile. To calculate values for the curves, equations 2 and 5 were arranged to calculate stress ratios for these quantiles. To establish a fair comparison and eliminate confusion, stress ratios for the Glaser model were modified by 5% to compensate for differing methods of accounting for pressurization rate. The rate difference is built into the Phoenix model, whereas the pressurization rate must be applied to the Orbiter vessels before using the

Glaser model. When these differing pressurization rate assumptions are accounted for, the differences in reliability estimates are very small; less than 1%.

To understand why the models provide results that are so similar requires an understanding of differences and similarities of the parameters used. Clearly equations 2 and 4 are similar and the simplification of equation 4 to equation 5 reveals the power-law structure of the Glaser model. To facilitate a comparison, the Glaser model is mapped onto the Phoenix model.

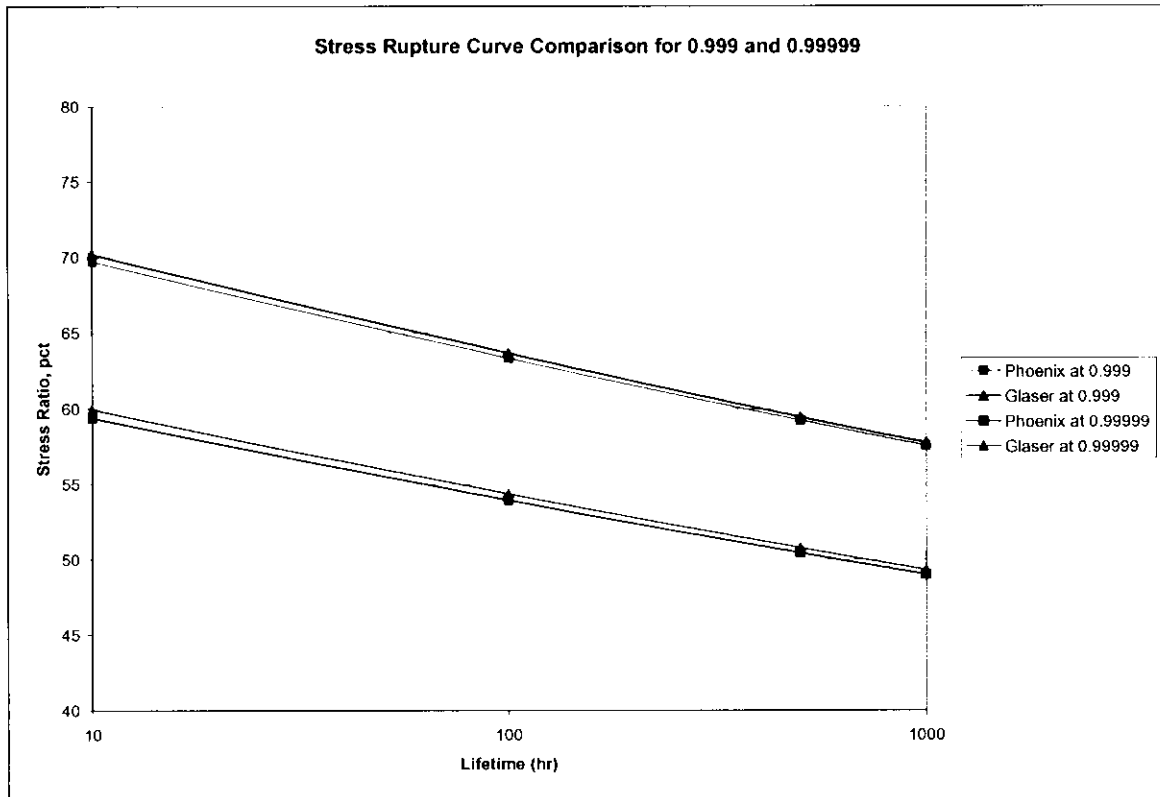


Figure 4. Stress Rupture curve comparison for probabilities of survival of 0.999 and 0.99999.

Rearranging the Glaser model (equation 5), we arrive at equation 7.

$$P\{T_s > t\} = \exp\left[-\left(\frac{t}{e^{\beta_1} s^{-\beta_2}}\right)^{1/\beta_3}\right] \quad (7)$$

Immediate parallels can be drawn between this form and equation 2:  $1/\beta_3$  must be equal to  $\beta$  and  $-\beta_2$  must be equal to  $\rho$ . A comparison of tables 1 and 2 reveal that this is true as summarized in table 4. However, parallels between the Glaser model and the Phoenix parameter of  $t_{c,ref}$  are more difficult. Accounting for differences between the definition of stress ratio by adding a factor,  $r$ , and determining the value of  $e^{\beta_1}$  allows this comparison as illustrated in equation 8.

$$P\{T_s > t\} = \exp\left[-\left(\frac{t}{e^{\beta_1} r^{\beta_2}} s^{-\beta_2}\right)^{1/\beta_3}\right] \quad (8)$$

In equation 8,  $r = \left(\frac{100}{0.95}\right)$ . This factor is needed because the Phoenix model accounts for a 5% pressurization rate effect in the LLNL data and the Glaser model defines stress ratio in terms of percentage of actual burst strength of LLNL vessels, as discussed previously. Calculating a value for  $e^{\beta_1} \cdot r$  from coefficients listed in table 2, a value very similar to  $t_{c,ref}$  is found as seen in table 4.

**Table 4. Parameter and Coefficient comparisons.**

Shape Parameter	$\beta$	1.2
	$1/\beta_3$	1.236
Power Law Exponent	$\rho$	24
	$-\beta_2$	23.602
Time reference	$t_{c,ref}$	0.5456
	$e^{\beta_1} \cdot r$	0.6275

The similarity of these models as evidenced by the similarities between parameter values is surprising since the models were derived using different approaches and the Glaser model had more adjustable parameters that might have provided a better and different fit to the LLNL data and thus, different predictions. These similarities in the behavior of the models lend credibility to both and to the reliability estimations for the Orbiter COPVs. Other models for stress rupture exist and will be explored in future publications.

### Confidence Intervals and Stress Rupture Parameter Sensitivities

The conditional probability of survival is a function of several variables and parameters which have been determined based on limited amounts of data. However, uncertainties do exist, and treating various parameters as deterministic variables and arriving at a single point probability of survival estimate number is hidden with dangers. In order to be able to account for the inherent uncertainties, one should consider the probabilistic aspects of the phenomenon in a more rigorous manner. Accordingly the point probability estimate becomes a random variable and hence one needs to bound this with either upper and lower confidence bounds or one sided confidence bounds. An attempt is made to capture these in the Phoenix and Glaser models and a comparison of the various methodologies is presented in this section.

Equation 9 is an expression for probability of survival in a generic form as a function of several pertinent random variables

$$P_S(\sigma, t) = F(\sigma_r, t_r, \Delta t_r, \rho, \beta) \quad (9)$$

where

$$\sigma_r = \frac{\sigma_l}{\sigma_{c,ref}}, \quad (10)$$

$$t_r = \frac{t_l}{t_{c,ref}}, \quad (11)$$

$$\Delta t_r = \frac{\Delta t_l}{t_{c,ref}} \quad (12)$$

The symbols  $\rho$ , and  $\beta$  are the power law coefficient and the shape factor respectively. A limit state function (sometimes referred to as performance function) is defined as:

$$g(\bar{X}) = P_S(\bar{X}) - P_{S0} \quad (13)$$

where  $P_{S0}$  is a particular value of  $P_S$ . The vector  $\bar{X}$  represents the various uncertain variables considered in the current problem. The limit state function can be an implicit or explicit function of random variables and is divided in such a way that  $g(\bar{X}) = 0$  is a boundary between the region  $[g \leq 0]$ , which means that a certain level of reliability is not met and  $[g > 0]$ , which means the reliability is met meeting or exceeded. It should be noted that since the cumulative distribution function (CDF) of  $P_S$  at  $P_{S0}$  equals the probability that  $[g \leq 0]$ , the CDF can be computed by varying  $P_{S0}$  and computing the point probability.

The probability that  $[g \leq 0]$ , is given by the integral

$$P[g \leq 0] = \int_{\Omega} f_X(X_1, X_2, \dots, X_n) dX_1 dX_2 \dots dX_n \quad (14)$$

in which  $f_X(X_1, X_2, \dots, X_n)$  is the joint probability density function for variables  $X_1, X_2 \dots X_n$  and the integration is performed over the region,  $\Omega$ , where  $g \leq 0$ . If the random variables are statistically independent, then the joint probability density function can be replaced by individual density functions. This integral can be computed by standard Monte Carlo procedure which is rather straightforward. However, depending upon the number of random variables involved and the level of  $P_{S0}$  sought, this must be repeated thousands of times, to accurately build the response variable's probabilistic characteristics. Although inherently simple, the large number of output sets that must be generated to build the CDF of the output variable, becomes its obvious disadvantage. Furthermore, if the deterministic computation of the response is complicated, time-consuming analysis (e.g. a large non-linear finite element analysis), the time required and the computational costs could become prohibitive.

In our present case, however, we have a closed form expression for the conditional probability for mission survival as given below<sup>19,20,21</sup>

$$P_S(t|\sigma_S(*), t_1) = \frac{\exp \left\{ - \left[ \left( \frac{t_1}{t_{c,ref}} \right) \left( \frac{\sigma_{op1}}{\sigma_{c,ref}} \right)^\rho + \left( \frac{\Delta t}{t_{c,ref}} \right) \left( \frac{\sigma_{op2}}{\sigma_{c,ref}} \right)^\rho \right]^\beta \right\}}{\exp \left\{ - \left[ \left( \frac{t_1}{t_{c,ref}} \right) \left( \frac{\sigma_{op1}}{\sigma_{c,ref}} \right)^\rho \right]^\beta \right\}} \quad (15)$$

Equation 15 is an un-simplified version of equation 3 and is solved using 1,000,000 Monte-Carlo simulations for each class of vehicle. These simulations were performed using the Southwest Research Institute developed code NESSUS ver. 8.2. Details of the theory are outlined in reference 22. The variables considered in the process are listed in Table 5. The survival probabilities for one sided 95% confidence limit are computed for each of the vessels and the results are tabulated in Table 6.

It should be noted that in the above calculations the four random variables are considered to be independent and therefore the resulting confidence limits will be pessimistically wider than the reality. One obvious dependency, for instance, is that since  $t_{c,ref}$  corresponds to a stress ratio of unity, whereas the stress ratio of interest is 0.575, and the data LLNL data itself spans the stress ratio 0.75 approximately, then an estimate on the low side for  $\rho$  will tend to be accompanied by a high estimate for  $t_{c,ref}$ , due to the pivot effect around 0.75 stress ratio and this will tend to compensate most of the effect of a low  $\rho$  value. The limits therefore can be considered to be on the conservative side. The correlation between the four variables must be taken in to account if more representative confidence limits are to be sought.

**Table 5. Input random variables and their values chosen for the current illustration.**

Random Variable	Distribution Type	Mean	Coef. Of Variation
$\sigma_{MOP}/\sigma_p$	Weibull	0.575	3%
$\rho$	Log Normal	24	5%
$\beta$	Log Normal	1.2	16%
$t_p$	Log Normal	.5457	5%

**Table 6. Survival probabilities based on 1,000,000 Monte Carlo simulations**

Vehicle Class	Probability of Survival 95% C.L.	Probability of Failure 95% C.L.
OMS-He	0.99895211	0.00104789
RCS-He	0.9998385	0.0001615
MPS-B-He	0.99994075	5.925E-05
MPS-S-He	0.99999726	2.74E-06
ECLSS-N2	0.9999805	1.95E-05

Furthermore, the coefficients of variation in the random variables considered are based on current best judgment. A reduction in the variance will give tighter confidence bounds.

A limited study of the deterministic sensitivity of the conditional probability of survival to various parameters of interest was also done and is reported in figure 5. Each variable is normalized with respect to the mean value and is varied one at a time between 0.4 to 1.4. From figure 6, it is clear that the conditional survival probability is most sensitive to variables stress ratio and the power law coefficient  $\rho$ , while it is fairly insensitive to the values of  $t_{c,ref}$  and  $\beta$ .

The results of confidence bounds estimations using various formulations is given along with the point probability of survival estimates in Table 7. Figure 6 shows a pictorial comparison of the probability of failure for each sub-system. In arriving at these results, the past effective times at pressure in hours for each COPV sub-system, as well as the current mission duration hours were best estimates at the time these results were computed. The past times for each of the 24 vessels were independently estimated and the highest number of hours for each COPV sub-system was considered in the calculations to be on conservative side. Since this study was done, based upon the NESC input, several operational as well as

other changes were brought in order to minimize the times spent with the view to maximize the reliability and life. As a result the most recent estimations for the hours differ slightly from those reported here. For the purpose of comparison of various models, however, these differences do not affect the qualitative conclusions of the study. Note that although the methodologies used for conditional probability are different in the Glaser and the Phoenix models, the predictions for point probability estimates as well as confidence limit estimates are virtually indistinguishable.

In addition to the present work, extensive discussion and analysis of confidence intervals has been undertaken by the NESC COPV team including Ron Glaser and Leigh Phoenix. It is unclear how confidence intervals can provide additional assurances of the future flightworthiness of the Orbiter COPVs. Discussion of findings and analyses of confidence interval approaches will be provided in future publications, but the results from the confidence interval determination developed by Glaser are shown in figure 6 for comparison with the present analysis.

**Table 7. A comparison of the two methodology predictions**

OV-103 COPV Sub-System	Conditional Probability of Survival/Phoenix	Conditional Probability of Survival/Ron Glaser	Phoenix-95%	Glaser-95%
OMS He	0.99984546	0.99985216	0.99895211	0.99872706
RCS He	0.99998602	0.99998753	0.9998385	0.99986917
MPS he	0.9999955	0.99999406	0.99994075	0.99993648
MPS He	0.99999992	0.99999993	0.99999726	0.99999887
ECLSS N2	0.99999887	0.99999892	0.9999805	0.99998654

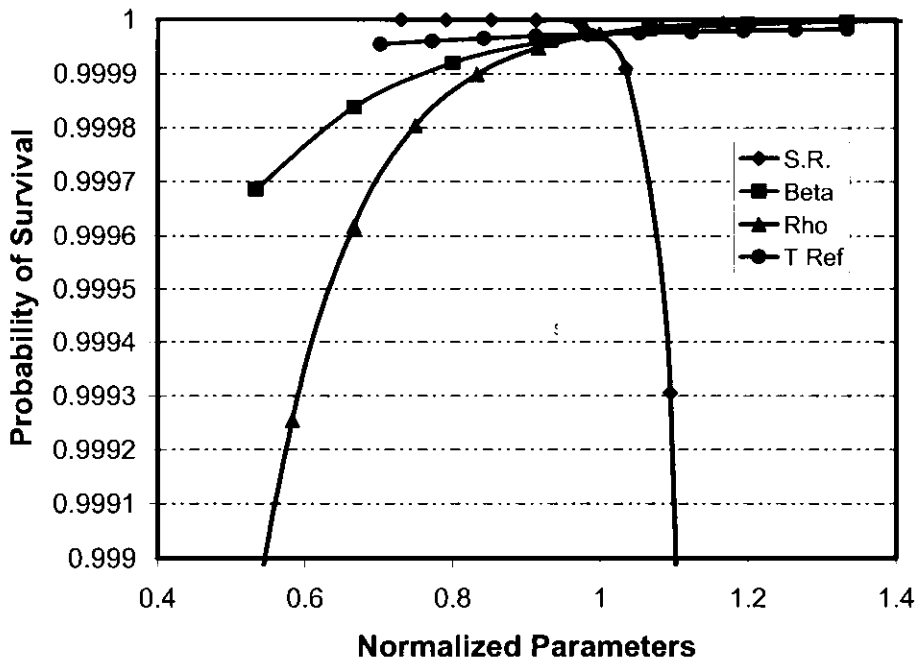


**Figure 5. Sensitivity of the conditional probability of survival to various normalized stress rupture life estimation parameters.**

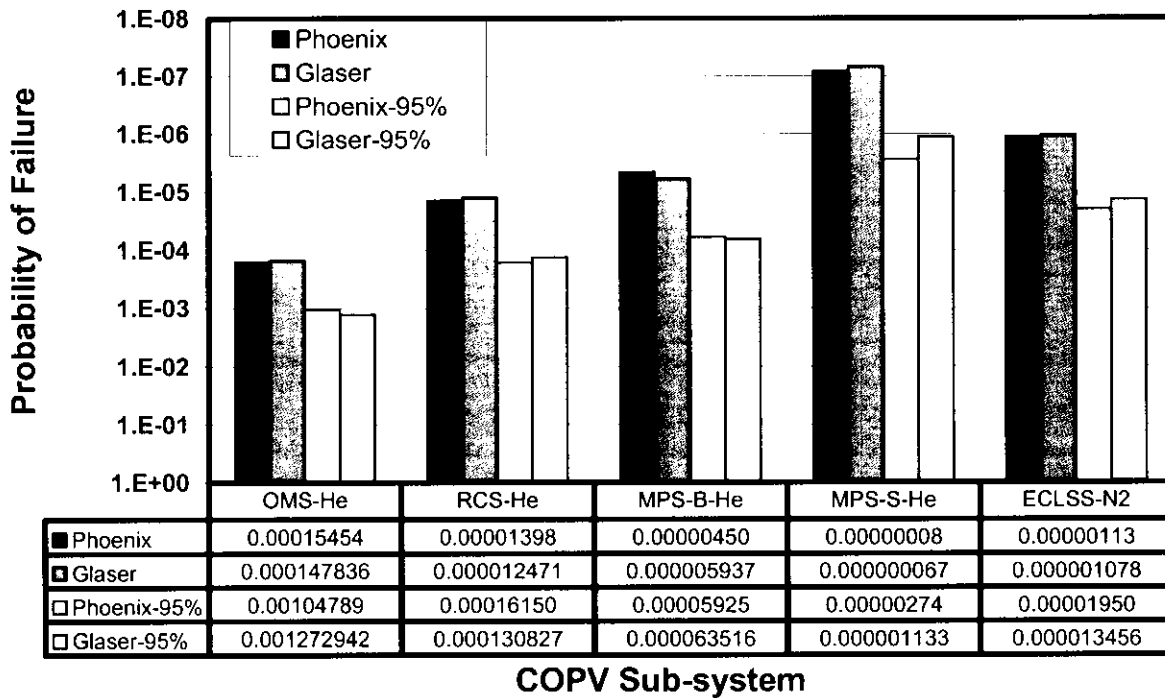


Figure 6. A comparison of all the three methodologies; point and 95% one sided confidence estimates for probability of failure for various COPV sub-systems.

### Conclusion

To provide an assessment of continued use of the 24 composite overwrapped pressure vessels on board the Orbiter, reliability estimates were provided by Phoenix and Glaser. These estimates are very similar despite differing approaches and this lends credibility to both models which were developed independently. Work is ongoing to understand uncertainty and the role of confidence intervals for future flights of the Orbiter. While work to revise current reliability point estimates is also ongoing, estimates available currently are low based on the Phoenix and Glaser models. Rationale for continued flight will be contingent upon further revision and mitigating actions.

### Glossary of Symbols:

$\sigma_{burst}$	Stress in fiber at burst pressure
$\sigma_{op}$	Stress in fiber at operating pressure
$\sigma_{op1}, \sigma_{op2}$	Stress in fiber at past/present operating pressures
$\sigma_{ref}$	Stress at reference time in the plateau region
$\rho$	Power law coefficient for stress in Phoenix model
$\beta$	Shape parameter
$\beta_1, \beta_2, \beta_3$	Coefficients based on maximum likelihood estimates in Glaser Model
$t$	Time

$t_1$	Past effective time in hours
$t_{c,ref}$	Reference time at the plateau region
$\alpha$	Scale parameter
$P$	Probability
$\Delta t$	Current mission time spent at operating stress ratio
$s$	Stress ratio used in the Glaser model
$r$	Correction factor to account for pressurization rate differences
$g(\underline{X})$	Limit state function
$\underline{X}$	Vector of uncertain variables
$f_x$	Joint probability density function
$\Omega$	Region of uncertain variables

## References

1. NESC Composite Overwrapped Pressure Vessel Independent Technical Assessment Final Report.
2. Glaser, R.E., R.L. Moore, and T.T. Chiao. "Life Estimation of an S-Glass/Epoxy Composite under Tensile Loading." *Composites Technical Review*, Vol. 5, No. 1 (1983): 21-26.
3. Glaser, R.E., R.L. Moore, and T.T. Chiao. "Life Estimation of Aramid/Epoxy Composites under Sustained Tension." *Composites Technical Review*, Vol. 26 (1984): 26.
4. Phoenix, S. Leigh, and E.M. Wu. "Statistics for The Time Dependent Failure of Kevlar-49/Epoxy Composites: Micromechanical Modeling and Data Interpretation." IUTAM Symposium on Mechanics of Composite Materials, Pergamon (1983):135.
5. Thomas, Donald. "Long-Life Assessment of Graphite/Epoxy Materials for Space Station Freedom Pressure Vessels." *Jet Propulsion*, Vol. 8, No. 1 (1992): 87.
6. Wagner, H.D., P. Schwartz, and S. Leigh Phoenix, "Lifetime Statistics for single Kevlar 49 filaments in creep-rupture." *J. Mat. Sci.*, Vol. 21 (1986):1868.
7. Wagner, H.D., S. Leigh Phoenix, and P. Schwartz. "A Study of Statistical Variability in the Strength of Single Aramid Filaments." *J. Comp. Mat'ls*, Vol. 18 (July 1984): 312.
8. Michalske, T.A., and B. Bunker. "A Chemical Kinetics Model for Glass Fracture." *Journal of American Ceramics Society*, Vol. 76, No. 10, (1993): 2613-18.
9. Phoenix, S. Leigh. "Statistical Modeling of the Time and Temperature Dependent Failure of Fibrous Composites." Proceedings of the 9th US National Congress of Applied Mechanics, Book # H00228, ASME, NY (1982): 219-229.
10. Christensen, R., "Interactive Mechanical and Chemical Degradation in Organic Materials", *Int. J. Solids Structures*, v. 20, No. 8, (1984)791.
11. Phoenix, S. Leigh, and I.J. Beyerlein. "Statistical Strength Theory for Fibrous Composite Materials." *Comprehensive Composite Materials*, Elsevier Science(2000): 1-81.
12. Glaser, R.E., R.L. Moore, and T.T. Chiao. "Life Estimation of Aramid/Epoxy Composites under Sustained Tension." *Composites Technical Review*, Vol. 26 (1984): 26-35.
13. Wagner, H.D., P. Schwartz, and S. Leigh Phoenix, "Lifetime Statistics for single Kevlar 49 filaments in creep-rupture." *J. Mat. Sci.*, Vol. 21 (1986):1868.
14. Glaser, R.E. "Statistical Analysis of Kevlar 49/Epoxy Composite Stress-Rupture Data." LLNL UCID-19849, Sept. 1983.
15. Glaser, R.E., R.L. Moore, and T.T. Chiao. "Life Estimation of Aramid/Epoxy Composites under Sustained Tension." *Composites Technical Review*, Vol. 26 (1984): 26-35.
16. Wu, H.F., S. Leigh Phoenix, and P. Schwartz. "Temperature Dependence of Lifetime Statistics for Single Kevlar 49 Filaments in Creep- Rupture." *Journal of Material Science*, Vol. 23 (1988):1851-1860.
17. Ibnabdeljalil, M., and S. Leigh Phoenix. "Creep Rupture of Brittle Matrix Composites Reinforced with Time Dependent Fibers: Scalings and Monte Carlo Simulations." *Journal of Mechanical Physical Solids*, Vol. 43, No. 6 (1995): 897-931.
18. Coleman, B., "Statistics and Time Dependent Mechanical Breakdown in Fibers", *J. Applied Physics*, v. 29, n. 6, 1958.
19. Methodology for determining reliability of Kevlar COPVs in future missions under reduced operating pressures, S. L. Phoenix, draft 4, April 10, 2005.

20. Update on Reliability Predictions from LLNL Kevlar COPVs (Including Effect of Vessel #188) and Confidence Interval Issues, S. L. Phoenix, June 13, 2005
21. Effect of Uncertainty in our Reliability Calculations, S.L. Phoenix, April 22, 2005
22. FPI User's and Theoretical Manuals, Southwest Research Institute, 1995.

FINAL  
06-0141

# A COMPARISON OF VARIOUS STRESS RUPTURE LIFE MODELS FOR ORBITER COMPOSITE PRESSURE VESSELS AND CONFIDENCE INTERVALS

Lorie Grimes-Ledesma  
Jet Propulsion Laboratory, California Institute of Technology

Pappu L.N. Murthy  
NASA Glenn Research Center

S. Leigh Phoenix  
Cornell University

Ronald Glaser  
Lawrence Livermore National Laboratory, University of California

In conjunction with a recent NASA Engineering and Safety Center (NESC) investigation of flight worthiness of Kevlar Overwrapped Composite Pressure Vessels (COPVs) on board the Orbiter, two stress rupture life prediction models were proposed independently by Phoenix and by Glaser. In this paper, the use of these models to determine the system reliability of 24 COPVs currently in service on board the Orbiter is discussed. The models are briefly described, compared to each other, and model parameters and parameter error are also reviewed to understand confidence in reliability estimation as well as the sensitivities of these parameters in influencing overall predicted reliability levels.

Differences and similarities in the various models will be compared via stress rupture reliability curves (stress ratio vs. lifetime plots). Also outlined will be the differences in the underlying model premises, and predictive outcomes. Sources of error and sensitivities in the models will be examined and discussed based on sensitivity analysis and confidence interval determination. Confidence interval results and their implications will be discussed for the models by Phoenix and Glaser.

## Stress Rupture as an Aging Orbiter Concern

Composite Overwrapped Pressure Vessels (COPVs) consist of a thin metallic liner overwrapped with a high strength filament wound composite. Because the composite carries the majority of the pressure load during operation, the amount of higher weight metallic structure needed is reduced. This results in a significantly lower mass pressure vessel as compared to an all-metallic vessel. The overall savings achieved based on the required 24 COPVs per Orbiter, was 700 lb. over monolithic titanium tanks.<sup>1</sup> On the Orbiter; these vessels are used for storing pressurant inert gases for propulsion systems (OMS- Orbital Maneuvering System, RCS- Reaction Control System, MPS- Main Propulsion System) and environmental systems (ECLSS- Environmental Control System). Locations of these COPVs on board the Orbiter are shown in Figure 1.

COPVs are susceptible to many of the same failure modes as metallic pressure vessels, but additional considerations are required to ensure that the vessel has a reliable composite overwrap. The majority of these composite failure modes were adequately mitigated during the design of the vessels, but a re-assessment of the stress rupture failure mode was necessary for the Orbiter COPVs because most of the COPVs had been in service since the beginning of the Shuttle program in the early 1980's.<sup>1</sup> This re-assessment was important because a COPV that fails due to the stress rupture failure mode will burst

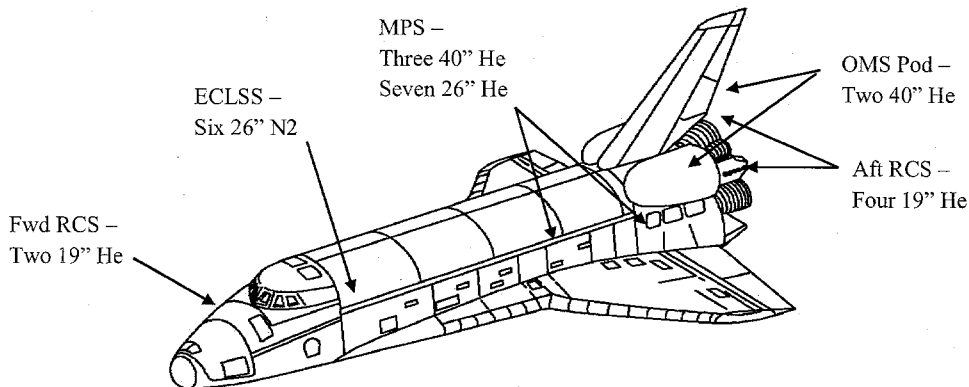


**Figure 1. Orbiter COPV locations.**

suddenly. A burst failure of any of the COPVs on board the Orbiter would likely have catastrophic results.

Stress rupture is the failure of a fiber as a function of sustained load and time. A COPV that fails due to the stress rupture failure mode will burst. It is understood mainly on a phenomenological level and stress rupture life prediction methodologies are based on stochastic modeling. The following have been repeatedly observed by many researchers.<sup>2-7</sup>

1. Stress rupture lifetime is mainly a function of composite fiber stress (usually expressed as a percentage of short-term strength, called the stress ratio).
2. Stress rupture is a material property of the fiber although matrix properties play a role in terms of influencing the mechanics of inter-fiber load sharing prior to catastrophic failure. Different fiber types (carbon, Kevlar, glass) have different stress rupture characteristics.
3. Stress rupture life data can be fit using Weibull statistics with a distribution function of the form:

$$P(s) = 1 - e^{-\left(\frac{x}{\alpha}\right)^\beta} \quad (1)$$

where  $x$  is stress,  $\alpha$  is the scale parameter and  $\beta$  is the shape parameter.

4. During room temperature testing, slow degradation of the fiber with time is not observed, i.e. the fiber appears to maintain its original strength until it suddenly fails, and thus, strength (burst) testing of aged composites cannot provide an indication of remaining stress rupture life (for tests at elevated temperatures, however, a reduction in burst strength has been observed for Kevlar).

Stress rupture of a composite is due to the failure of the fiber. At present, no single mechanism has been proven definitively as the leading cause for failure in Kevlar or carbon, although for glass, a water-based stress-corrosion mechanism has been demonstrated.<sup>8</sup> For Kevlar, chain scission/slippage models and time-dependent continuum crack growth models have been suggested, but the parameters in the end must be established empirically.<sup>9,10</sup> Ties between fiber stress rupture failure and the overall failure of the

composite have been analytically studied. A progressive failure model has been developed by Phoenix, and others at Cornell, based on a progression beginning with chain scission/slippage within the fiber prior to the failure of adjacent fibers and shear failure of the resin leading to fiber break cluster growth and failure of the composite.<sup>9</sup> Since load transfer to other fibers occurs through shear transfer in the resin during the failure of a composite, the resin does have an effect on the stress rupture life, but the effect is not first order for Kevlar fiber at typical operating stress levels. Matrix effects are more significant in the case of carbon fibers.<sup>11</sup>

Stress rupture life testing for Kevlar has been performed primarily by Lawrence Livermore National Laboratory (LLNL) and Cornell University with Kevlar material characterization contributions from the Y12 Plant at Oak Ridge National Laboratory and Sandia National Laboratories. These tests have consisted of single-fiber, fiber-bundle, resin impregnated strand (or tow tests), and COPV testing at a single constant stress level.<sup>12-15</sup> Although most of this testing has been conducted at ambient temperature, temperature acceleration has been performed to decrease the stress rupture life based on the concept that scission rate increases with temperature. Testing of this idea was performed at LLNL and Cornell.<sup>16</sup>

Although models based on data from LLNL, Cornell, and DOE are available in the literature, they are not directly comparable to any other COPV design as published. For the purposes of evaluation of the Orbiter COPVs, the pressure vessel data developed at LLNL were used because this data most closely resembles the structure of the Orbiter COPVs. However, modifications to the data as published were required. Changes were made to account for the load carrying effects of the liner, the effects of strength variations between different spools used to overwrap the COPVs, and compensation for differences in ultimate burst strength of the composite due to differences in pressurization rate between the Orbiter COPVs and LLNL test COPVs. In addition to these a small correction to account for Kevlar creep relaxation was also applied.

The establishment of a relationship between the very-different designs of the LLNL test COPVs and the Orbiter vessels was non-trivial and was a major thrust of the study. The development of relationships between burst strength, composite operational stress level, and fiber quantity were necessary. Detailed discussion of these relationships will be reported elsewhere.

To determine the continued flightworthiness of Orbiter COPVs, the NESC sponsored a study of forecasts based on independently derived models for stress rupture. Since Leigh Phoenix at Cornell University, Ron Glaser at Lawrence Livermore National Laboratory (LLNL), and Ernest Robinson at the Aerospace Corporation had already established independent frameworks for the modeling of stress rupture of Kevlar as evidenced in academic literature over the past 30 years or so, they were chosen to provide stress rupture life models to the NESC for the Orbiter COPVs. The Phoenix and Glaser models will be discussed and compared in this paper although the model of Robinson has equal merit and will be discussed in detail in a future publication.

### **Phoenix Model**

The Phoenix model has been developed over the past 27 years and is well documented in the literature. It is based on a Weibull distribution framework for strength and lifetime with the embodiment of a power law to describe damage in a composite versus stress level. Derivation of the model is available in references 9 and 17, where the power-law in stress level (with temperature dependence) is derived from thermally activated chain scission using a Morse potential as a model. While the basic concepts for the model are the same as those previously developed, the parameters are based on an entirely new analysis of the LLNL pressure vessel data. Though not discussed here, the model has also been applied to strand data as well, with comparable results. In the simplest setting of constant stress applied quickly and maintained over a long time period, the basic equation for the model is below.

$$P(t, \sigma) = 1 - \exp \left[ - \left\{ \left( \frac{t}{t_{c,ref}} \right) \left( \frac{\sigma_{op}}{\sigma_{burst}} \right)^\rho \right\}^\beta \right] \quad (2)$$

The ratio of  $\sigma_{op}/\sigma_{burst}$  is the ratio of fiber stress at operating pressure to fiber stress at burst pressure (stress ratio),  $t$  is time,  $t_{c,ref}$  is a reference time,  $\rho$  is the power law exponent, and  $\beta$  is the Weibull shape parameter for lifetime. The value for  $\sigma_{burst}$  accounts for pressurization rate differences between Orbiter COPVs and the LLNL test COPVs. This strain rate effect has been discussed in reference 4 and will be discussed in later publications in more detail. The strain rate difference between Orbiter COPVs and LLNL test COPVs is inherent in the Phoenix model because the stress ratios for the LLNL vessel data have been modified to account for this rate. The model is shown for a single stress level over time, but for more general time histories a memory integral is used to accumulate damage (similar to Miner's rule for fatigue) at different stress levels. Also, at very high stress levels a second quantity within square brackets and of similar structure to the first must also be included with a leading minus sign as well (i.e., in a weakest damage mechanism framework). This second quantity has different parameter values, especially a much higher  $\rho$  value.

In the Phoenix model, values for the parameters  $t_{c,ref}$ ,  $\rho$ , and  $\beta$  are determined based on the LLNL vessel data and are influenced by observations of stress rupture behavior of strands and single fibers. Values for these parameters determined by Phoenix for the LLNL vessel data are shown in Table 1. The power law exponent,  $\rho$ , is the inverse of the slope of the logs of the scale parameter of the stress rupture data and the stress ratio. The parameter  $t_{c,ref}$  is an anchor point determined from this slope and an instantaneous reference strength. In the Phoenix model, both  $\rho$  and  $\beta$  are based primarily on the LLNL vessel data but were chosen such that all data available (which includes data from other Kevlar COPVs and strands) are considered. In this way the parameters are determined from broader observations of stress rupture data as a whole, making the resulting reliability estimations consistent with all stress rupture data. This "big picture" approach is a unique feature of the Phoenix model.

**Table 1. Parameter values for the Phoenix model.**

Parameter	Value
$\rho$	24
$\beta$	1.2
$t_{c,ref}$	0.5456

Based on the Phoenix model, a series of reliability quantile curves can be developed for use in design that allow estimation of the lifetime for a chosen quantile. Figure 2 shows the stress rupture curve for the Phoenix model. This approach can be used by choosing an appropriate combination of stress ratio and lifetime to ensure a desired reliability during the design of a COPV. Analysis based on this approach is employed currently by COPV manufacturers.

However, in the case of the Orbiter, the COPVs had been successfully operated for a long period of time already, so a conditional probability approach was used (in essence ruling out unusually short lived vessels within the population since none actually occurred). In this approach, a reference time is chosen and all successful history prior to the reference is considered in the analysis. In the case of the Orbiter vessels, the reference time was chosen as return-to-flight. Because the vessels had successfully "survived" up to the reference time this successful past history is credited in the analysis. The conditional reliability equation for the Phoenix model is below.

$$F(t, \sigma) = 1 - \exp \left[ - \left\{ \left( \frac{t_1}{t_{c,ref}} \right) \left( \frac{\sigma_{op1}}{\sigma_{ref}} \right)^\rho + \frac{\Delta t}{t_{c,ref}} \left( \frac{\sigma_{op2}}{\sigma_{ref}} \right)^\rho \right\}^\beta + \left( \frac{t_1}{t_{c,ref}} \left( \frac{\sigma_{op1}}{\sigma_{ref}} \right)^\rho \right)^\beta \right] \quad (3)$$

In this equation, two new terms appear, one for a second stress level and another to account for past history. This conditional reliability equation was used in all Phoenix calculations for Orbiter reliability estimates for future flights.

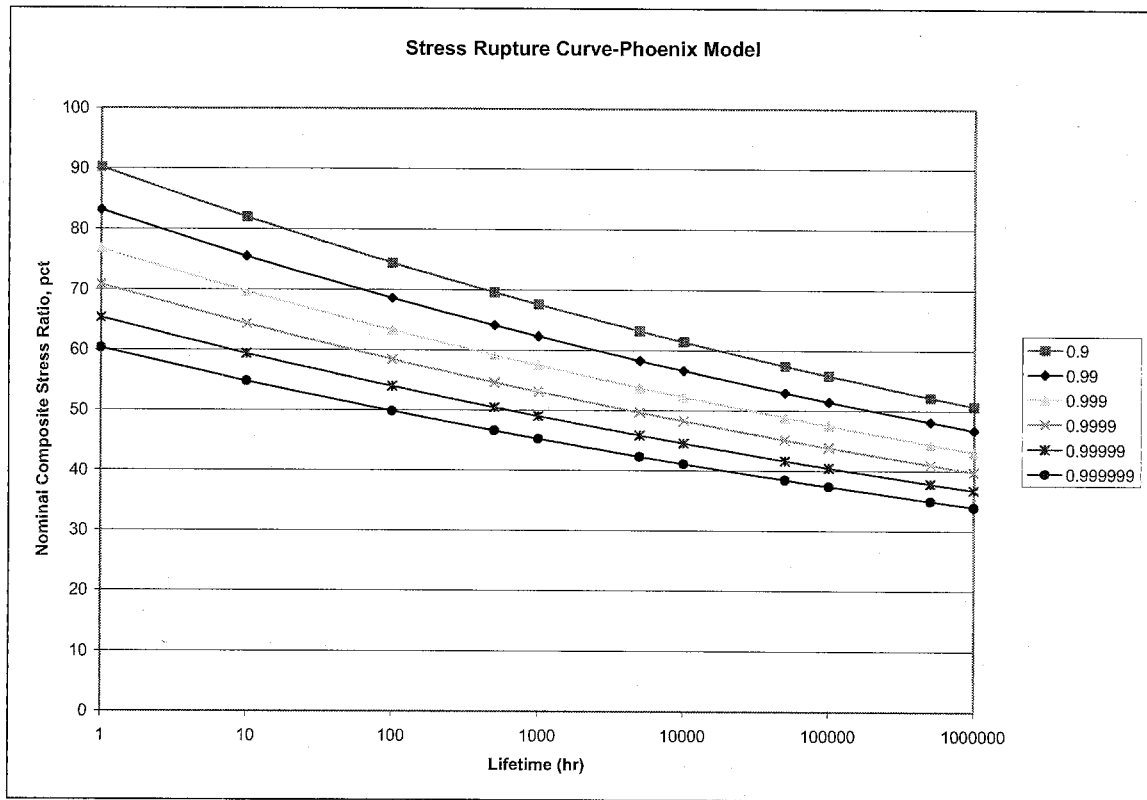


Figure 2. Phoenix Stress Rupture Curve. Quantiles are for probability of survival.

### Glaser Model

The Glaser model was developed independently of the Phoenix model during the same time frame and is also based on a Weibull distribution with a generalized power law. The equation for the survival probability in the Glaser model is below.

$$P\{T_s > t\} = \exp \left[ - \left( \frac{t}{a(s)} \right)^{b(s)} \right] \quad (4)$$

where

$$\alpha(s) = \log a(s) = \beta_1 + \beta_2 \log s$$

$$\sigma(s) = 1/b(s) = \beta_3$$

The model simplifies to:

$$P\{T_s > t\} = \exp\left[-\left(\frac{t}{e^{\beta_1 s^{\beta_2}}}\right)^{1/\beta_3}\right] \quad (5)$$

In the Glaser model,  $s$  is the stress ratio, and the  $\beta$ 's are coefficients based on the LLNL vessel data. Unlike the Phoenix model, no strain rate adjustments were applied to the LLNL vessel burst strengths to account for strain rate differences relative to the LLNL vessels.

In the model, the  $\beta$  values are determined based on a maximum likelihood methodology developed by Glaser and are shown for the LLNL COPV data in Table 2.

**Table 2. Coefficient values for the Glaser model.**

Parameter	Value
$\beta_1$	109.4367
$\beta_2$	-23.602
$\beta_3$	0.8088

While the form of the Glaser model is similar to that presented in the literature and in LLNL reports<sup>2,14</sup>, estimation of  $\alpha(s)$  and  $\sigma(s)$  was changed to allow a comparison with the Orbiter COPVs. The original forms had a stress varying shape parameter -  $b(s)$ , which was a polynomial function of stress ratio, rather than a constant. The model was changed to a constant shape parameter to focus the model in the center of the data to minimize the effect of the data at lower and upper tails of the distribution and extremes of stress ratio.

As discussed previously, the model can be represented graphically in a set of stress rupture curves. Glaser was the originator of this representational method and curves based on his model are shown in figure 3. While these curves are applicable to the Orbiter COPVs, curves based on previous versions of the Glaser model are not directly applicable to the Orbiter COPVs.

Although these stress rupture curves provide an expedient method of determining reliability during design, Glaser also chose a conditional reliability approach for the Orbiter COPVs. The conditional reliability version of the Glaser model is below.

$$M(s, t, s^*, \Delta) = 1 - P\{T_{s^*} > t^* + \Delta \mid T_{s^*} > t^*\} = 1 - \exp\left[-\left(\frac{t^* + \Delta}{e^{\beta_1 s^* \beta_2}}\right)^{1/\beta_3} + \left(\frac{t^*}{e^{\beta_1 s^* \beta_2}}\right)^{1/\beta_3}\right] \quad (6)$$

In this formula, another term is created to account for the successful past history of the Orbiter COPVs. This conditional reliability equation was used in all Glaser calculations for Orbiter reliability estimates for future flights.

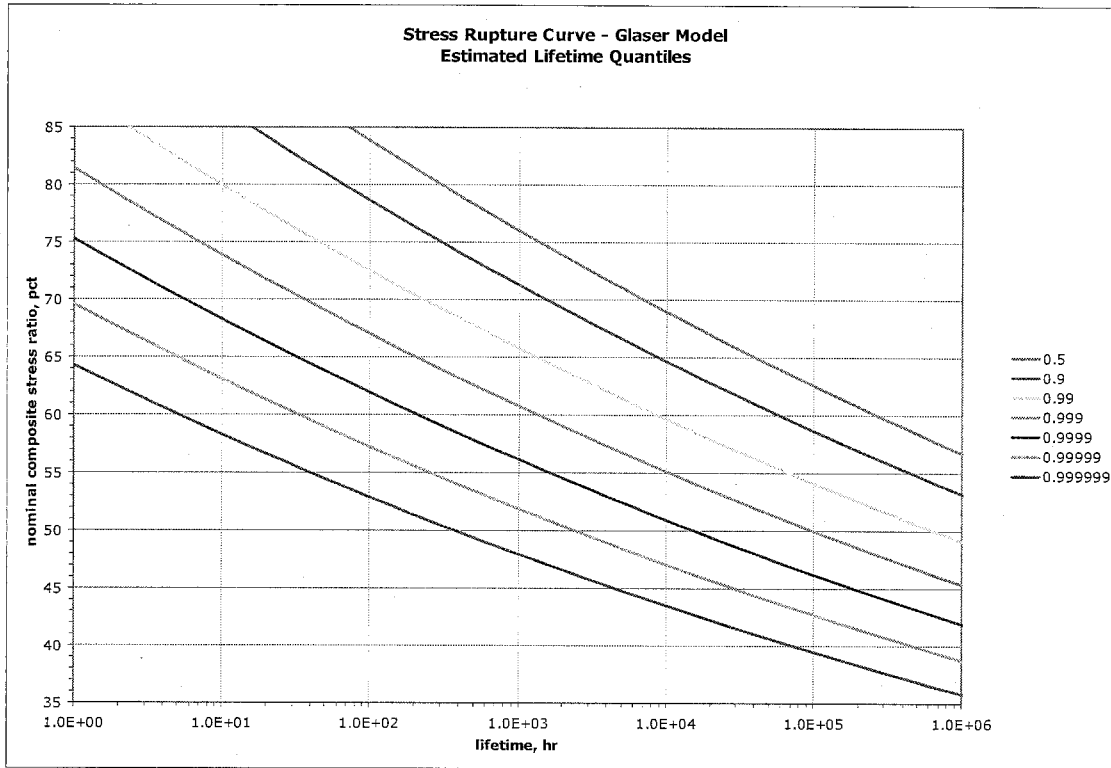


Figure 3. Glaser Stress Rupture Curve. Quantiles are for probability of survival.

### Comparison of Reliability Models from Glaser and Phoenix

Both the Phoenix and Glaser models are based on a power-law framework within the Weibull distribution. This methodology has a basis in early composites failure theory developed by Coleman.<sup>18</sup> The models provide virtually indistinguishable reliability estimates for the Orbiter COPVs, especially when conditional reliability is used. A comparison between results for each model is shown in table 3.

Table 3. Comparison of Reliability Estimates for Using Phoenix and Glaser Models. Estimates are calculated for the next scheduled flight.

Vessel Type	Stress Ratio for Phoenix Model	Stress Ratio for Glaser Model	Past Accumulated Hours	Hours for One Future Mission	No. of Vessels	Non-Conditional		Conditional		
						Phoenix	Glaser	Phoenix	Glaser	
OMS	0.575	0.604	4151	252	1	0.994571361	0.995182204	0.99960116	0.99899579	
OMS	0.575	0.604	3983	252	1	0.994833253	0.99542157	0.99960434	0.99899579	
RCS	0.515	0.541	7551	630	2	0.999066453	0.999187175	0.99990573	0.99962693	
RCS	0.515	0.541	6620	395	2	0.999202759	0.999309176	0.99994256	0.99976608	
RCS	0.515	0.541	6112	249	2	0.999275571	0.999374093	0.99996443	0.99985253	
MPS he	0.54	0.576	858	24	3	0.999596528	0.999483792	0.99998642	0.99990638	
MPS He	0.47	0.494	858	24	7	0.999982728	0.999986366	0.99999942	0.99999418	
ECLSS N2-1	0.445	0.468	74495	648	1	0.999891619	0.999899715	0.99999887	0.99999373	
ECLSS N2-2	0.445	0.468	74495	648	1	0.999891619	0.999899715	0.99999887	0.99999373	
ECLSS N2-3	0.445	0.468	74408	648	1	0.999891771	0.999899859	0.99999887	0.99999373	
ECLSS N2-4	0.445	0.468	65910	648	1	0.999906428	0.999913803	0.99999889	0.99999373	
ECLSS N2-5	0.445	0.468	61793	648	1	0.999913397	0.999920409	0.99999891	0.99999373	
ECLSS N2-6	0.445	0.468	22548	648	1	0.999974169	0.999977116	0.99999911	0.99999373	
<b>Reliability for Entire System of COPVs=</b>							0.986066333	0.987510562	0.99899791	0.99710314

Table 3 shows the probability of survival estimates using the basic models (non-conditional) and conditional reliability models. For each of the vessel types, the reliability is determined as a function of the number of vessels in that type, so it's the single vessel reliability to the number of vessels of that type. To determine the overall system level reliability, the reliabilities of each vessel type are multiplied to arrive at a reliability estimate for the Orbiter system of COPVs. This similarity of the results despite their independent development lends credibility to both models.

A more general comparison of the basic models is observed in stress rupture curve comparisons. Figure 4 shows a stress rupture curve for the 0.999 and 0.99999 quantile. To calculate values for the curves, equations 2 and 5 were arranged to calculate stress ratios for these quantiles. To establish a fair comparison and eliminate confusion, stress ratios for the Glaser model were modified by 5% to compensate for differing methods of accounting for pressurization rate. The rate difference is built into the Phoenix model, whereas the pressurization rate must be applied to the Orbiter vessels before using the Glaser model. When these differing pressurization rate assumptions are accounted for, the differences in reliability estimates are very small; less than 1%.

To understand why the models provide results that are so similar requires an understanding of differences and similarities of the parameters used. Clearly equations 2 and 4 are similar and the simplification of equation 4 to equation 5 reveals the power-law structure of the Glaser model. To facilitate a comparison, the Glaser model is mapped onto the Phoenix model.

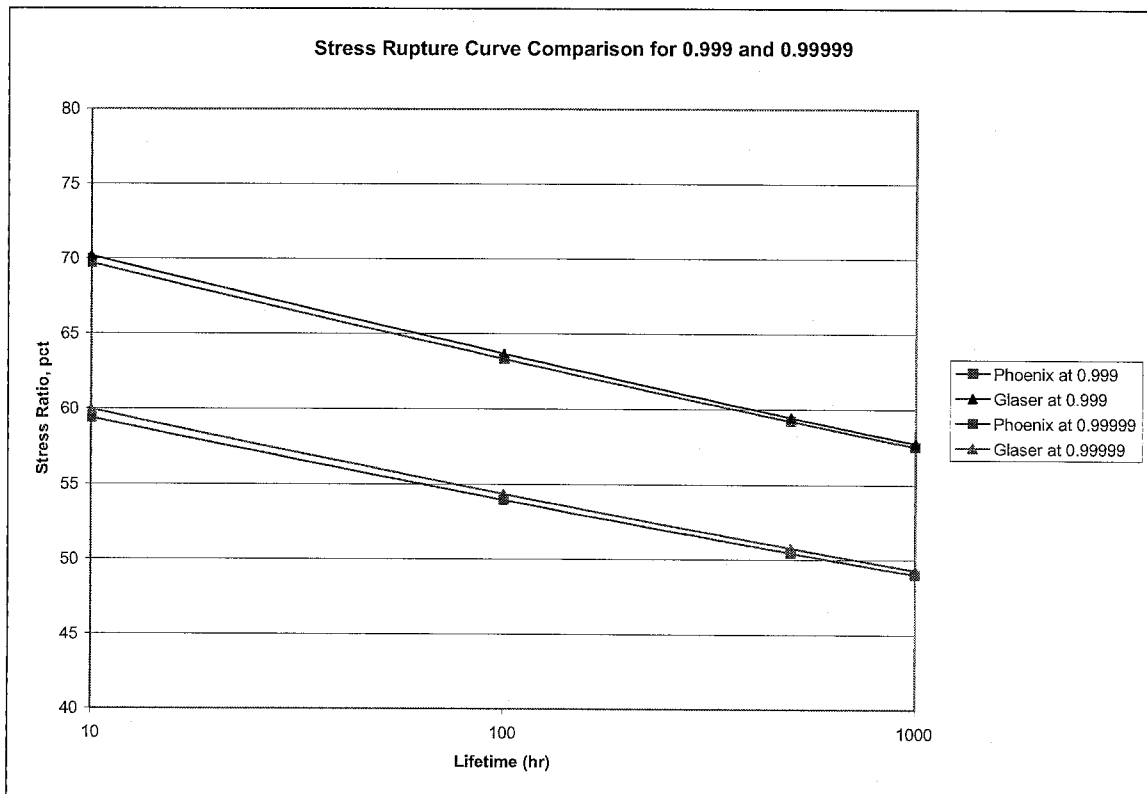


Figure 4. Stress Rupture curve comparison for probabilities of survival of 0.999 and 0.99999.

Rearranging the Glaser model (equation 5), we arrive at equation 7.

$$P\{T_s > t\} = \exp\left[-\left(\frac{t}{e^{\beta_1} s^{-\beta_2}}\right)^{1/\beta_3}\right] \quad (7)$$

Immediate parallels can be drawn between this form and equation 2:  $1/\beta_3$  must be equal to  $\beta$  and  $-\beta_2$  must be equal to  $\rho$ . A comparison of tables 1 and 2 reveal that this is true as summarized in table 4. However, parallels between the Glaser model and the Phoenix parameter of  $t_{c,ref}$  are more difficult. Accounting for differences between the definition of stress ratio by adding a factor,  $r$ , and determining the value of  $e^{\beta_1}$  allows this comparison as illustrated in equation 8.

$$P\{T_s > t\} = \exp\left[-\left(\frac{t}{e^{\beta_1} r^{\beta_2} s^{-\beta_2}}\right)^{1/\beta_3}\right] \quad (8)$$

In equation 8,  $r = \left(\frac{100}{0.95}\right)$ . This factor is needed because the Phoenix model accounts for a 5% pressurization rate effect in the LLNL data and the Glaser model defines stress ratio in terms of percentage of actual burst strength of LLNL vessels, as discussed previously. Calculating a value for  $e^{\beta_1} \cdot r$  from coefficients listed in table 2, a value very similar to  $t_{c,ref}$  is found as seen in table 4.

**Table 4. Parameter and Coefficient comparisons.**

Shape	$\beta$	1.2
Parameter	$1/\beta_3$	1.236
Power Law Exponent	$\rho$	24
	$-\beta_2$	23.602
Time reference	$t_{c,ref}$	0.5456
	$e^{\beta_1} \cdot r$	0.6275

The similarity of these models as evidenced by the similarities between parameter values is surprising since the models were derived using different approaches and the Glaser model had more adjustable parameters that might have provided a better and different fit to the LLNL data and thus, different predictions. These similarities in the behavior of the models lend credibility to both and to the reliability estimations for the Orbiter COPVs. Other models for stress rupture exist and will be explored in future publications.

### Confidence Intervals and Stress Rupture Parameter Sensitivities

The conditional probability of survival is a function of several variables and parameters which have been determined based on limited amounts of data. However, uncertainties do exist, and treating various parameters as deterministic variables and arriving at a single point probability of survival estimate number is hidden with dangers. In order to be able to account for the inherent uncertainties, one should consider the probabilistic aspects of the phenomenon in a more rigorous manner. Accordingly the point probability estimate becomes a random variable and hence one needs to bound this with either upper and

lower confidence bounds or one sided confidence bounds. An attempt is made to capture these in the Phoenix and Glaser models and a comparison of the various methodologies is presented in this section.

Equation 9 is an expression for probability of survival in a generic form as a function of several pertinent random variables

$$P_S(\sigma, t) = F(\sigma_R, t_R, \Delta t_R, \rho, \beta) \quad (9)$$

where

$$\sigma_R = \frac{\sigma_1}{\sigma_{c,ref}}, \quad (10)$$

$$t_R = \frac{t_1}{t_{c,ref}}, \quad (11)$$

$$\Delta t_R = \frac{\Delta t_1}{t_{c,ref}} \quad (12)$$

The symbols  $\rho$ , and  $\beta$  are the power law coefficient and the shape factor respectively.

A limit state function (sometimes referred to as performance function) is defined as:

$$g(\bar{X}) = P_S(\bar{X}) - P_{S0} \quad (13)$$

where  $P_{S0}$  is a particular value of  $P_S$ . The vector  $\bar{X}$  represents the various uncertain variables considered in the current problem. The limit state function can be an implicit or explicit function of random variables and is divided in such a way that  $g(\bar{X}) = 0$  is a boundary between the region  $[g \leq 0]$ , which means that a certain level of reliability is not met and  $[g > 0]$ , which means the reliability is met meeting or exceeded. It should be noted that since the cumulative distribution function (CDF) of  $P_S$  at  $P_{S0}$  equals the probability that  $[g \leq 0]$ , the CDF can be computed by varying  $P_{S0}$  and computing the point probability.

The probability that  $[g \leq 0]$ , is given by the integral

$$P[g \leq 0] = \int_{\Omega} \dots \int f_X(X_1, X_2, \dots, X_n) dX_1 dX_2 \dots dX_n \quad (14)$$

in which  $f_X(X_1, X_2, \dots, X_n)$  is the joint probability density function for variables  $X_1, X_2 \dots X_n$  and the integration is performed over the region,  $\Omega$ , where  $g \leq 0$ . If the random variables are statistically independent, then the joint probability density function can be replaced by individual density functions. This integral can be computed by standard Monte Carlo procedure which is rather straightforward. However, depending upon the number of random variables involved and the level of  $P_{S0}$  sought, this must be repeated thousands of times, to accurately build the response variable's probabilistic characteristics. Although inherently simple, the large number of output sets that must be generated to build the CDF of the output variable, becomes its obvious disadvantage. Furthermore, if the deterministic computation of

the response is complicated, time-consuming analysis (e.g. a large non-linear finite element analysis), the time required and the computational costs could become prohibitive.

In our present case, however, we have a closed form expression for the conditional probability for mission survival as given below<sup>19,20,21</sup>

$$P_S(t|\sigma_S(*), t_1) = \frac{\exp \left\{ - \left[ \left( \frac{t_1}{t_{c,ref}} \right) \left( \frac{\sigma_{op1}}{\sigma_{c,ref}} \right)^\rho + \left( \frac{\Delta t}{t_{c,ref}} \right) \left( \frac{\sigma_{op2}}{\sigma_{c,ref}} \right)^\rho \right]^\beta \right\}}{\exp \left\{ - \left[ \left( \frac{t_1}{t_{c,ref}} \right) \left( \frac{\sigma_{op1}}{\sigma_{c,ref}} \right)^\rho \right]^\beta \right\}} \quad (15)$$

Equation 15 is an un-simplified version of equation 3 and is solved using 1,000,000 Monte-Carlo simulations for each class of vehicle. These simulations were performed using the Southwest Research Institute developed code NESSUS ver. 8.2. Details of the theory are outlined in reference 22. The variables considered in the process are listed in Table 5. The survival probabilities for one sided 95% confidence limit are computed for each of the vessels and the results are tabulated in Table 6.

It should be noted that in the above calculations the four random variables are considered to be independent and therefore the resulting confidence limits will be pessimistically wider than the reality. One obvious dependency, for instance, is that since  $t_{c,ref}$  corresponds to a stress ratio of unity, whereas the stress ratio of interest is 0.575, and the data LLNL data itself spans the stress ratio 0.75 approximately, then an estimate on the low side for  $\rho$  will tend to be accompanied by a high estimate for  $t_{c,ref}$  due to the pivot effect around 0.75 stress ratio and this will tend to compensate most of the effect of a low  $\rho$  value. The limits therefore can be considered to be on the conservative side. The correlation between the four variables must be taken in to account if more representative confidence limits are to be sought.

**Table 5. Input random variables and their values chosen for the current illustration.**

Random Variable	Distribution Type	Mean	Coef. Of Variation
$\sigma_{MOP}/\sigma_p$	Weibull	0.575	3%
$\rho$	Log Normal	24	5%
$\beta$	Log Normal	1.2	16%
$t_p$	Log Normal	.5457	5%

**Table 6. Survival probabilities based on 1,000,000 Monte Carlo simulations**

Vehicle Class	Probability of Survival 95% C.L	Probability of Failure 95% C.L.
OMS-He	0.99895211	0.00104789
RCS-He	0.9998385	0.0001615
MPS-B-He	0.99994075	5.925E-05
MPS-S-He	0.99999726	2.74E-06
ECLSS-N2	0.9999805	1.95E-05

Furthermore, the coefficients of variation in the random variables considered are based on current best judgment. A reduction in the variance will give tighter confidence bounds.

A limited study of the deterministic sensitivity of the conditional probability of survival to various parameters of interest was also done and is reported in figure 5. Each variable is normalized with respect to the mean value and is varied one at a time between 0.4 to 1.4. From figure 6, it is clear that the conditional survival probability is most sensitive to variables stress ratio and the power law coefficient  $\rho$ , while it is fairly insensitive to the values of  $t_{c,ref}$ , and  $\beta$ .

The results of confidence bounds estimations using various formulations is given along with the point probability of survival estimates in Table 7. Figure 6 shows a pictorial comparison of the probability of failure for each sub-system. In arriving at these results, the past effective times at pressure in hours for each COPV sub-system, as well as the current mission duration hours were best estimates at the time these results were computed. The past times for each of the 24 vessels were independently estimated and the highest number of hours for each COPV sub-system was considered in the calculations to be on conservative side. Since this study was done, based upon the NESC input, several operational as well as other changes were brought in order to minimize the times spent with the view to maximize the reliability and life. As a result the most recent estimations for the hours differ slightly from those reported here. For the purpose of comparison of various models, however, these differences do not affect the qualitative conclusions of the study. Note that although the methodologies used for conditional probability are different in the Glaser and the Phoenix models, the predictions for point probability estimates as well as confidence limit estimates are virtually indistinguishable.

In addition to the present work, extensive discussion and analysis of confidence intervals has been undertaken by the NESC COPV team including Ron Glaser and Leigh Phoenix. It is unclear how confidence intervals can provide additional assurances of the future flightworthiness of the Orbiter COPVs. Discussion of findings and analyses of confidence interval approaches will be provided in future publications, but the results from the confidence interval determination developed by Glaser are shown in figure 6 for comparison with the present analysis.

**Table 7. A comparison of the two methodology predictions**

<b>OV-103 COPV Sub- System</b>	<b>Conditional Probability of Survival/ Phoenix</b>	<b>Conditional Probability of Survival/ Ron Glaser</b>	<b>Phoenix- 95%</b>	<b>Glaser- 95%</b>
<b>OMS He</b>	<b>0.99984546</b>	<b>0.99985216</b>	<b>0.99895211</b>	<b>0.99872706</b>
<b>RCS He</b>	<b>0.99998602</b>	<b>0.99998753</b>	<b>0.9998385</b>	<b>0.99986917</b>
<b>MPS he</b>	<b>0.9999955</b>	<b>0.99999406</b>	<b>0.99994075</b>	<b>0.99993648</b>
<b>MPS He</b>	<b>0.99999992</b>	<b>0.99999993</b>	<b>0.99999726</b>	<b>0.99999887</b>
<b>ECLSS N2</b>	<b>0.99999887</b>	<b>0.99999892</b>	<b>0.9999805</b>	<b>0.99998654</b>

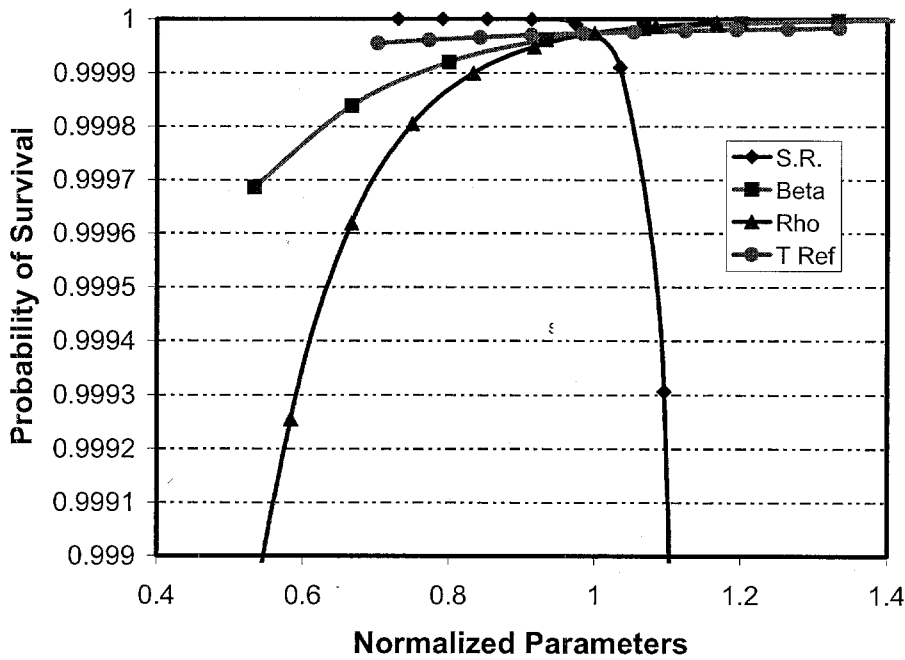
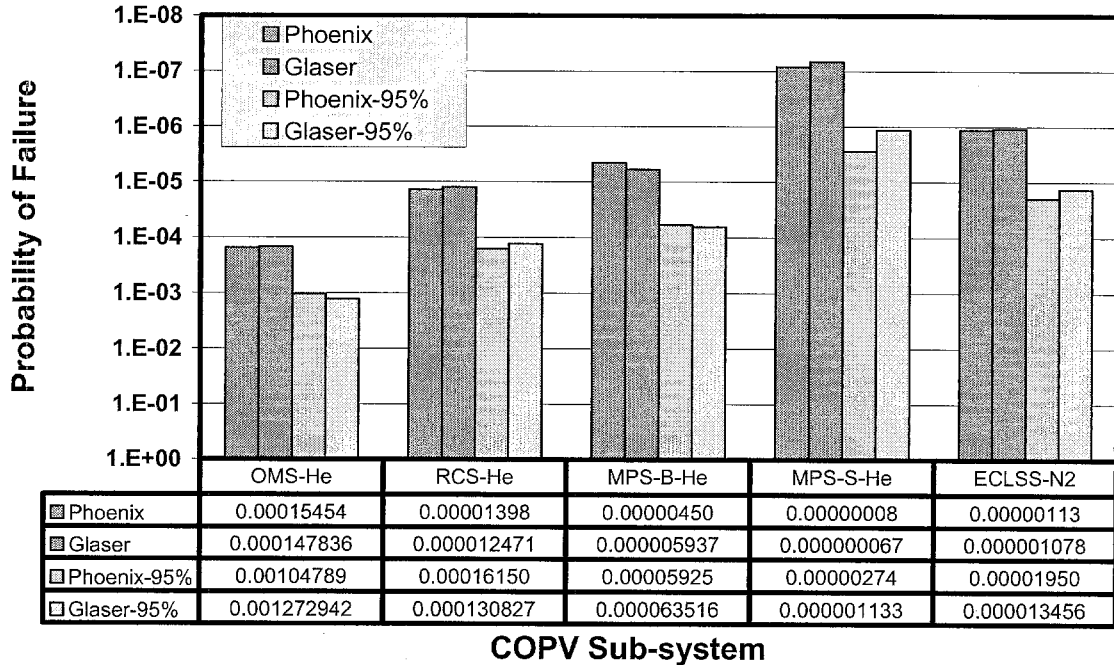


Figure 5. Sensitivity of the conditional probability of survival to various normalized stress rupture life estimation parameters.



**Figure 6. A comparison of all the three methodologies; point and 95% one sided confidence estimates for probability of failure for various COPV sub-systems.**

## Conclusion

To provide an assessment to justify continued use of the 24 composite overwrapped pressure vessels on board the Orbiter, stress rupture reliability estimates were provided by Phoenix and Glaser. These estimates are very similar despite differing approaches and this lends credibility to both models which were developed independently. Work is ongoing to understand uncertainty and the role of confidence intervals for future flights of the Orbiter. While work to revise current reliability point estimates is also ongoing, estimates available currently are low based on the Phoenix and Glaser models. Rationale for continued flight will be contingent upon further revision and mitigating actions.

## Glossary of Symbols:

$\sigma_{burst}$	Stress in fiber at burst pressure
$\sigma_{op}$	Stress in fiber at operating pressure
$\sigma_{op1}, \sigma_{op2}$	Stress in fiber at past/present operating pressures
$\sigma_{ref}$	Stress at reference time in the plateau region
$\rho$	Power law coefficient for stress in Phoenix model
$\beta$	Shape parameter
$\beta_1, \beta_2, \beta_3$	Coefficients based on maximum likelihood estimates in Glaser Model
$t$	Time
$t_1$	Past effective time in hours
$t_{c,ref}$	Reference time at the plateau region
$\alpha$	Scale parameter
$P$	Probability
$\Delta t$	Current mission time spent at operating stress ratio
$s$	Stress ratio used in the Glaser model
$r$	Correction factor to account for pressurization rate differences
$g(\underline{X})$	Limit state function
$\underline{X}$	Vector of uncertain variables
$f_x$	Joint probability density function
$\Omega$	Region of uncertain variables

## References

1. NESC Composite Overwrapped Pressure Vessel Independent Technical Assessment Final Report.
2. Glaser, R.E., R.L. Moore, and T.T. Chiao. "Life Estimation of an S-Glass/Epoxy Composite under Tensile Loading." *Composites Technical Review*, Vol. 5, No. 1 (1983): 21-26.
3. Glaser, R.E., R.L. Moore, and T.T. Chiao. "Life Estimation of Aramid/Epoxy Composites under Sustained Tension." *Composites Technical Review*, Vol. 26 (1984): 26.
4. Phoenix, S. Leigh, and E.M. Wu. "Statistics for The Time Dependent Failure of Kevlar-49/Epoxy Composites: Micromechanical Modeling and Data Interpretation." IUTAM Symposium on Mechanics of Composite Materials, Pergamon (1983):135.
5. Thomas, Donald. "Long-Life Assessment of Graphite/Epoxy Materials for Space Station Freedom Pressure Vessels." *Jet Propulsion*, Vol. 8, No. 1 (1992): 87.
6. Wagner, H.D., P. Schwartz, and S. Leigh Phoenix, "Lifetime Statistics for single Kevlar 49 filaments in creep-rupture." *J. Mat. Sci.*, Vol. 21 (1986):1868.
7. Wagner, H.D., S. Leigh Phoenix, and P. Schwartz. "A Study of Statistical Variability in the Strength of Single Aramid Filaments." *J. Comp. Mat'ls*, Vol. 18 (July 1984): 312.

8. Michalske, T.A., and B. Bunker. "A Chemical Kinetics Model for Glass Fracture." *Journal of American Ceramics Society*, Vol. 76, No. 10, (1993): 2613-18.
9. Phoenix, S. Leigh. "Statistical Modeling of the Time and Temperature Dependent Failure of Fibrous Composites." Proceedings of the 9th US National Congress of Applied Mechanics, Book # H00228, ASME, NY (1982): 219-229.
10. Christensen, R., "Interactive Mechanical and Chemical Degradation in Organic Materials", *Int. J. Solids Structures*, v. 20, No. 8, (1984)791.
11. Phoenix, S. Leigh, and I.J. Beyerlein. "Statistical Strength Theory for Fibrous Composite Materials." *Comprehensive Composite Materials*, Elsevier Science(2000): 1-81.
12. Glaser, R.E., R.L. Moore, and T.T. Chiao. "Life Estimation of Aramid/Epoxy Composites under Sustained Tension." *Composites Technical Review*, Vol. 26 (1984): 26-35.
13. Wagner, H.D., P. Schwartz, and S. Leigh Phoenix, "Lifetime Statistics for single Kevlar 49 filaments in creep-rupture." *J. Mat. Sci.*, Vol. 21 (1986):1868.
14. Glaser, R.E. "Statistical Analysis of Kevlar 49/Epoxy Composite Stress-Rupture Data." LLNL UCID-19849, Sept. 1983.
15. Glaser, R.E., R.L. Moore, and T.T. Chiao. "Life Estimation of Aramid/Epoxy Composites under Sustained Tension." *Composites Technical Review*, Vol. 26 (1984): 26-35.
16. Wu, H.F., S. Leigh Phoenix, and P. Schwartz. "Temperature Dependence of Lifetime Statistics for Single Kevlar 49 Filaments in Creep- Rupture." *Journal of Material Science*, Vol. 23 (1988):1851-1860.
17. Ibnabdeljalil, M., and S. Leigh Phoenix. "Creep Rupture of Brittle Matrix Composites Reinforced with Time Dependent Fibers: Scalings and Monte Carlo Simulations." *Journal of Mechanical Physical Solids*, Vol. 43, No. 6 (1995): 897-931.
18. Coleman, B., "Statistics and Time Dependent Mechanical Breakdown in Fibers", *J. Applied Physics*, v. 29, n. 6, 1958.
19. Methodology for determining reliability of Kevlar COPVs in future missions under reduced operating pressures, S. L. Phoenix, draft 4, April 10, 2005.
20. Update on Reliability Predictions from LLNL Kevlar COPVs (Including Effect of Vessel #188) and Confidence Interval Issues, S. L. Phoenix, June 13, 2005
21. Effect of Uncertainty in our Reliability Calculations, S.L. Phoenix, April 22, 2005
22. FPI User's and Theoretical Manuals, Southwest Research Institute, 1995.

A portion of the research described in this (publication or paper) was carried out at the Jet Propulsion Laboratory, California Institute of Technology, under a contract with the National Aeronautics and Space Administration.

# A COMPARISON OF VARIOUS STRESS RUPTURE LIFE MODELS FOR ORBITER COMPOSITE PRESSURE VESSELS AND CONFIDENCE INTERVALS

FINAL

Lorie Grimes-Ledesma  
Jet Propulsion Laboratory, California Institute of Technology

Pappu L.N. Murthy  
NASA Glenn Research Center

S. Leigh Phoenix  
Cornell University

Ronald Glaser  
Lawrence Livermore National Laboratory, University of California

In conjunction with a recent NASA Engineering and Safety Center (NESC) investigation of flight worthiness of Kevlar Overwrapped Composite Pressure Vessels (COPVs) on board the Orbiter, two stress rupture life prediction models were proposed independently by Phoenix and by Glaser. In this paper, the use of these models to determine the system reliability of 24 COPVs currently in service on board the Orbiter is discussed. The models are briefly described, compared to each other, and model parameters and parameter error are also reviewed to understand confidence in reliability estimation as well as the sensitivities of these parameters in influencing overall predicted reliability levels.

Differences and similarities in the various models will be compared via stress rupture reliability curves (stress ratio vs. lifetime plots). Also outlined will be the differences in the underlying model premises, and predictive outcomes. Sources of error and sensitivities in the models will be examined and discussed based on sensitivity analysis and confidence interval determination. Confidence interval results and their implications will be discussed for the models by Phoenix and Glaser.

## Stress Rupture as an Aging Orbiter Concern

Composite Overwrapped Pressure Vessels (COPVs) consist of a thin metallic liner overwrapped with a high strength filament wound composite. Because the composite carries the majority of the pressure load during operation, the amount of higher weight metallic structure needed is reduced. This results in a significantly lower mass pressure vessel as compared to an all-metallic vessel. The overall savings achieved based on the required 24 COPVs per Orbiter, was 700 lb. over monolithic titanium tanks.<sup>1</sup> On the Orbiter; these vessels are used for storing pressurant inert gases for propulsion systems (OMS- Orbital Maneuvering System, RCS- Reaction Control System, MPS- Main Propulsion System) and environmental systems (ECLSS- Environmental Control System). Locations of these COPVs on board the Orbiter are shown in Figure 1.

COPVs are susceptible to many of the same failure modes as metallic pressure vessels, but additional considerations are required to ensure that the vessel has a reliable composite overwrap. The majority of these composite failure modes were adequately mitigated during the design of the vessels, but a re-assessment of the stress rupture failure mode was necessary for the Orbiter COPVs because most of the COPVs had been in service since the beginning of the Shuttle program in the early 1980's.<sup>1</sup> This re-assessment was important because a COPV that fails due to the stress rupture failure mode will burst

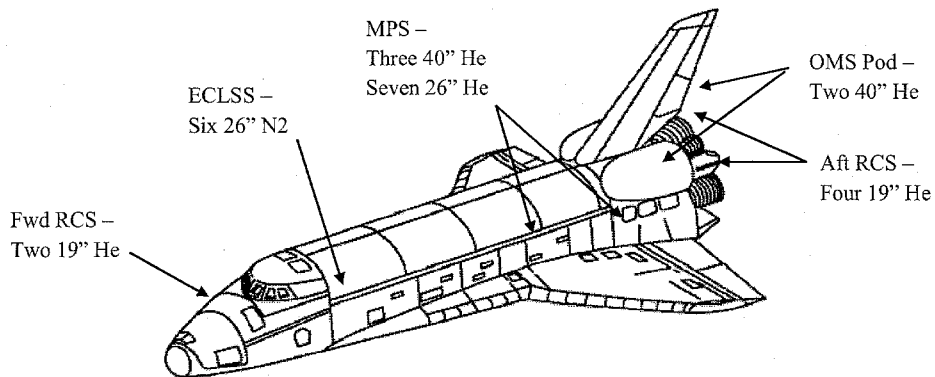


**Figure 1. Orbiter COPV locations.**

suddenly. A burst failure of any of the COPVs on board the Orbiter would likely have catastrophic results.

Stress rupture is the failure of a fiber as a function of sustained load and time. A COPV that fails due to the stress rupture failure mode will burst. It is understood mainly on a phenomenological level and stress rupture life prediction methodologies are based on stochastic modeling. The following have been repeatedly observed by many researchers.<sup>2-7</sup>

1. Stress rupture lifetime is mainly a function of composite fiber stress (usually expressed as a percentage of short-term strength, called the stress ratio).
2. Stress rupture is a material property of the fiber although matrix properties play a role in terms of influencing the mechanics of inter-fiber load sharing prior to catastrophic failure. Different fiber types (carbon, Kevlar, glass) have different stress rupture characteristics.
3. Stress rupture life data can be fit using Weibull statistics with a distribution function of the form:

$$P(s) = 1 - e^{-\left(\frac{x}{\alpha}\right)^\beta} \quad (1)$$

where  $x$  is stress,  $\alpha$  is the scale parameter and  $\beta$  is the shape parameter.

4. During room temperature testing, slow degradation of the fiber with time is not observed, i.e. the fiber appears to maintain its original strength until it suddenly fails, and thus, strength (burst) testing of aged composites cannot provide an indication of remaining stress rupture life (for tests at elevated temperatures, however, a reduction in burst strength has been observed for Kevlar).

Stress rupture of a composite is due to the failure of the fiber. At present, no single mechanism has been proven definitively as the leading cause for failure in Kevlar or carbon, although for glass, a water-based stress-corrosion mechanism has been demonstrated.<sup>8</sup> For Kevlar, chain scission/slippage models and time-dependent continuum crack growth models have been suggested, but the parameters in the end must be established empirically.<sup>9,10</sup> Ties between fiber stress rupture failure and the overall failure of the

composite have been analytically studied. A progressive failure model has been developed by Phoenix, and others at Cornell, based on a progression beginning with chain scission/slippage within the fiber prior to the failure of adjacent fibers and shear failure of the resin leading to fiber break cluster growth and failure of the composite.<sup>9</sup> Since load transfer to other fibers occurs through shear transfer in the resin during the failure of a composite, the resin does have an effect on the stress rupture life, but the effect is not first order for Kevlar fiber at typical operating stress levels. Matrix effects are more significant in the case of carbon fibers.<sup>11</sup>

Stress rupture life testing for Kevlar has been performed primarily by Lawrence Livermore National Laboratory (LLNL) and Cornell University with Kevlar material characterization contributions from the Y12 Plant at Oak Ridge National Laboratory and Sandia National Laboratories. These tests have consisted of single-fiber, fiber-bundle, resin impregnated strand (or tow tests), and COPV testing at a single constant stress level.<sup>12-15</sup> Although most of this testing has been conducted at ambient temperature, temperature acceleration has been performed to decrease the stress rupture life based on the concept that scission rate increases with temperature. Testing of this idea was performed at LLNL and Cornell.<sup>16</sup>

Although models based on data from LLNL, Cornell, and DOE are available in the literature, they are not directly comparable to any other COPV design as published. For the purposes of evaluation of the Orbiter COPVs, the pressure vessel data developed at LLNL were used because this data most closely resembles the structure of the Orbiter COPVs. However, modifications to the data as published were required. Changes were made to account for the load carrying effects of the liner, the effects of strength variations between different spools used to overwrap the COPVs, and compensation for differences in ultimate burst strength of the composite due to differences in pressurization rate between the Orbiter COPVs and LLNL test COPVs. In addition to these a small correction to account for Kevlar creep relaxation was also applied.

The establishment of a relationship between the very-different designs of the LLNL test COPVs and the Orbiter vessels was non-trivial and was a major thrust of the study. The development of relationships between burst strength, composite operational stress level, and fiber quantity were necessary. Detailed discussion of these relationships will be reported elsewhere.

To determine the continued flightworthiness of Orbiter COPVs, the NESC sponsored a study of forecasts based on independently derived models for stress rupture. Since Leigh Phoenix at Cornell University, Ron Glaser at Lawrence Livermore National Laboratory (LLNL), and Ernest Robinson at the Aerospace Corporation had already established independent frameworks for the modeling of stress rupture of Kevlar as evidenced in academic literature over the past 30 years or so, they were chosen to provide stress rupture life models to the NESC for the Orbiter COPVs. The Phoenix and Glaser models will be discussed and compared in this paper although the model of Robinson has equal merit and will be discussed in detail in a future publication.

### **Phoenix Model**

The Phoenix model has been developed over the past 27 years and is well documented in the literature. It is based on a Weibull distribution framework for strength and lifetime with the embodiment of a power law to describe damage in a composite versus stress level. Derivation of the model is available in references 9 and 17, where the power-law in stress level (with temperature dependence) is derived from thermally activated chain scission using a Morse potential as a model. While the basic concepts for the model are the same as those previously developed, the parameters are based on an entirely new analysis of the LLNL pressure vessel data. Though not discussed here, the model has also been applied to strand data as well, with comparable results. In the simplest setting of constant stress applied quickly and maintained over a long time period, the basic equation for the model is below.

$$P(t, \sigma) = 1 - \exp \left[ - \left\{ \left( \frac{t}{t_{c,ref}} \right) \left( \frac{\sigma_{op}}{\sigma_{burst}} \right)^\rho \right\}^\beta \right] \quad (2)$$

The ratio of  $\sigma_{op}/\sigma_{burst}$  is the ratio of fiber stress at operating pressure to fiber stress at burst pressure (stress ratio),  $t$  is time,  $t_{c,ref}$  is a reference time,  $\rho$  is the power law exponent, and  $\beta$  is the Weibull shape parameter for lifetime. The value for  $\sigma_{burst}$  accounts for pressurization rate differences between Orbiter COPVs and the LLNL test COPVs. This strain rate effect has been discussed in reference 4 and will be discussed in later publications in more detail. The strain rate difference between Orbiter COPVs and LLNL test COPVs is inherent in the Phoenix model because the stress ratios for the LLNL vessel data have been modified to account for this rate. The model is shown for a single stress level over time, but for more general time histories a memory integral is used to accumulate damage (similar to Miner's rule for fatigue) at different stress levels. Also, at very high stress levels a second quantity within square brackets and of similar structure to the first must also be included with a leading minus sign as well (i.e., in a weakest damage mechanism framework). This second quantity has different parameter values, especially a much higher  $\rho$  value.

In the Phoenix model, values for the parameters  $t_{c,ref}$ ,  $\rho$ , and  $\beta$  are determined based on the LLNL vessel data and are influenced by observations of stress rupture behavior of strands and single fibers. Values for these parameters determined by Phoenix for the LLNL vessel data are shown in Table 1. The power law exponent,  $\rho$ , is the inverse of the slope of the logs of the scale parameter of the stress rupture data and the stress ratio. The parameter  $t_{c,ref}$  is an anchor point determined from this slope and an instantaneous reference strength. In the Phoenix model, both  $\rho$  and  $\beta$  are based primarily on the LLNL vessel data but were chosen such that all data available (which includes data from other Kevlar COPVs and strands) are considered. In this way the parameters are determined from broader observations of stress rupture data as a whole, making the resulting reliability estimations consistent with all stress rupture data. This "big picture" approach is a unique feature of the Phoenix model.

**Table 1. Parameter values for the Phoenix model.**

Parameter	Value
$\rho$	24
$\beta$	1.2
$t_{c,ref}$	0.5456

Based on the Phoenix model, a series of reliability quantile curves can be developed for use in design that allow estimation of the lifetime for a chosen quantile. Figure 2 shows the stress rupture curve for the Phoenix model. This approach can be used by choosing an appropriate combination of stress ratio and lifetime to ensure a desired reliability during the design of a COPV. Analysis based on this approach is employed currently by COPV manufacturers.

However, in the case of the Orbiter, the COPVs had been successfully operated for a long period of time already, so a conditional probability approach was used (in essence ruling out unusually short lived vessels within the population since none actually occurred). In this approach, a reference time is chosen and all successful history prior to the reference is considered in the analysis. In the case of the Orbiter vessels, the reference time was chosen as return-to-flight. Because the vessels had successfully "survived" up to the reference time this successful past history is credited in the analysis. The conditional reliability equation for the Phoenix model is below.

$$F(t, \sigma) = 1 - \exp \left[ - \left\{ \left( \frac{t_1}{t_{c,ref}} \right) \left( \frac{\sigma_{op1}}{\sigma_{ref}} \right)^\rho + \frac{\Delta t}{t_{c,ref}} \left( \frac{\sigma_{op2}}{\sigma_{ref}} \right)^\rho \right\}^\beta + \left( \frac{t_1}{t_{c,ref}} \left( \frac{\sigma_{op1}}{\sigma_{ref}} \right)^\rho \right)^\beta \right] \quad (3)$$

In this equation, two new terms appear, one for a second stress level and another to account for past history. This conditional reliability equation was used in all Phoenix calculations for Orbiter reliability estimates for future flights.

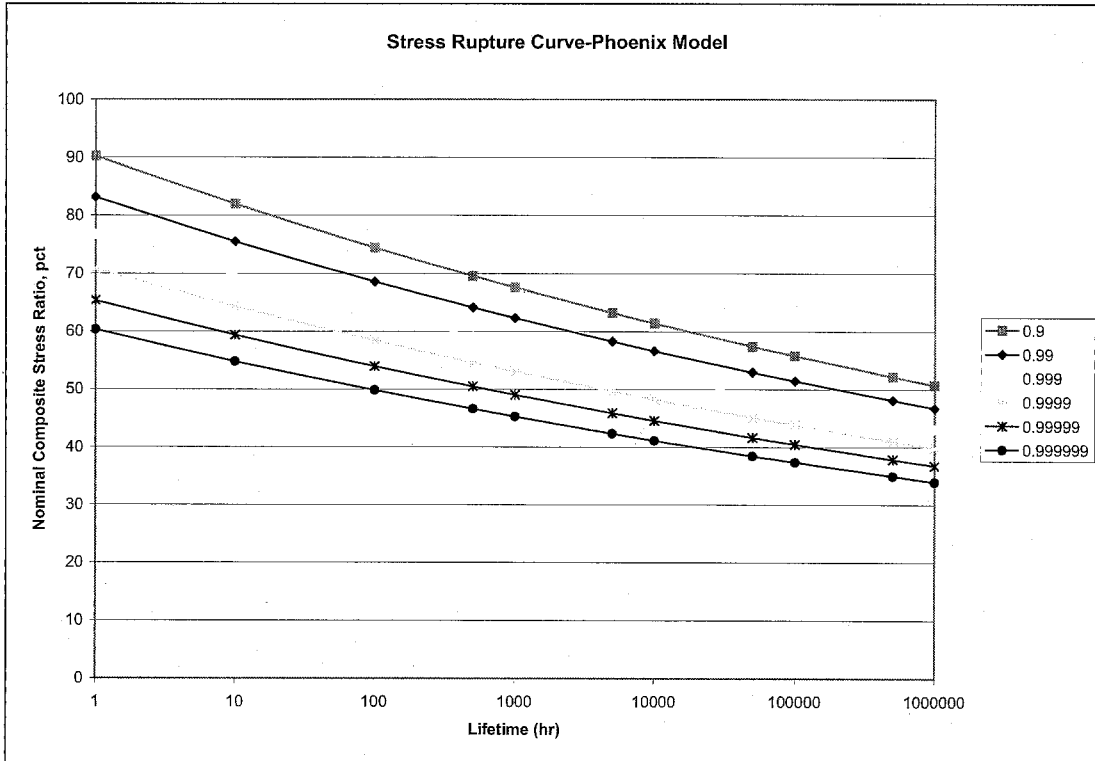


Figure 2. Phoenix Stress Rupture Curve. Quantiles are for probability of survival.

### Glaser Model

The Glaser model was developed independently of the Phoenix model during the same time frame and is also based on a Weibull distribution with a generalized power law. The equation for the survival probability in the Glaser model is below.

$$P\{T_s > t\} = \exp \left[ - \left( \frac{t}{a(s)} \right)^{b(s)} \right] \quad (4)$$

$$\text{where } \alpha(s) = \log a(s) = \beta_1 + \beta_2 \log s$$

$$\sigma(s) = 1/b(s) = \beta_3$$

The model simplifies to:

$$P\{T_s > t\} = \exp\left[-\left(\frac{t}{e^{\beta_1} s^{\beta_2}}\right)^{1/\beta_3}\right] \quad (5)$$

In the Glaser model,  $s$  is the stress ratio, and the  $\beta$ 's are coefficients based on the LLNL vessel data. Unlike the Phoenix model, no strain rate adjustments were applied to the LLNL vessel burst strengths to account for strain rate differences relative to the LLNL vessels.

In the model, the  $\beta$  values are determined based on a maximum likelihood methodology developed by Glaser and are shown for the LLNL COPV data in Table 2.

**Table 2. Coefficient values for the Glaser model.**

Parameter	Value
$\beta_1$	109.4367
$\beta_2$	-23.602
$\beta_3$	0.8088

While the form of the Glaser model is similar to that presented in the literature and in LLNL reports<sup>2,14</sup>, estimation of  $\alpha(s)$  and  $\sigma(s)$  was changed to allow a comparison with the Orbiter COPVs. The original forms had a stress varying shape parameter -  $b(s)$ , which was a polynomial function of stress ratio, rather than a constant. The model was changed to a constant shape parameter to focus the model in the center of the data to minimize the effect of the data at lower and upper tails of the distribution and extremes of stress ratio.

As discussed previously, the model can be represented graphically in a set of stress rupture curves. Glaser was the originator of this representational method and curves based on his model are shown in figure 3. While these curves are applicable to the Orbiter COPVs, curves based on previous versions of the Glaser model are not directly applicable to the Orbiter COPVs.

Although these stress rupture curves provide an expedient method of determining reliability during design, Glaser also chose a conditional reliability approach for the Orbiter COPVs. The conditional reliability version of the Glaser model is below.

$$M(s, t, s^*, \Delta) = 1 - P\{T_{s^*} > t^* + \Delta \mid T_{s^*} > t^*\} = 1 - \exp\left[-\left(\frac{t^* + \Delta}{e^{\beta_1} s^* \beta_2}\right)^{1/\beta_3} + \left(\frac{t^*}{e^{\beta_1} s^* \beta_2}\right)^{1/\beta_3}\right] \quad (6)$$

In this formula, another term is created to account for the successful past history of the Orbiter COPVs. This conditional reliability equation was used in all Glaser calculations for Orbiter reliability estimates for future flights.

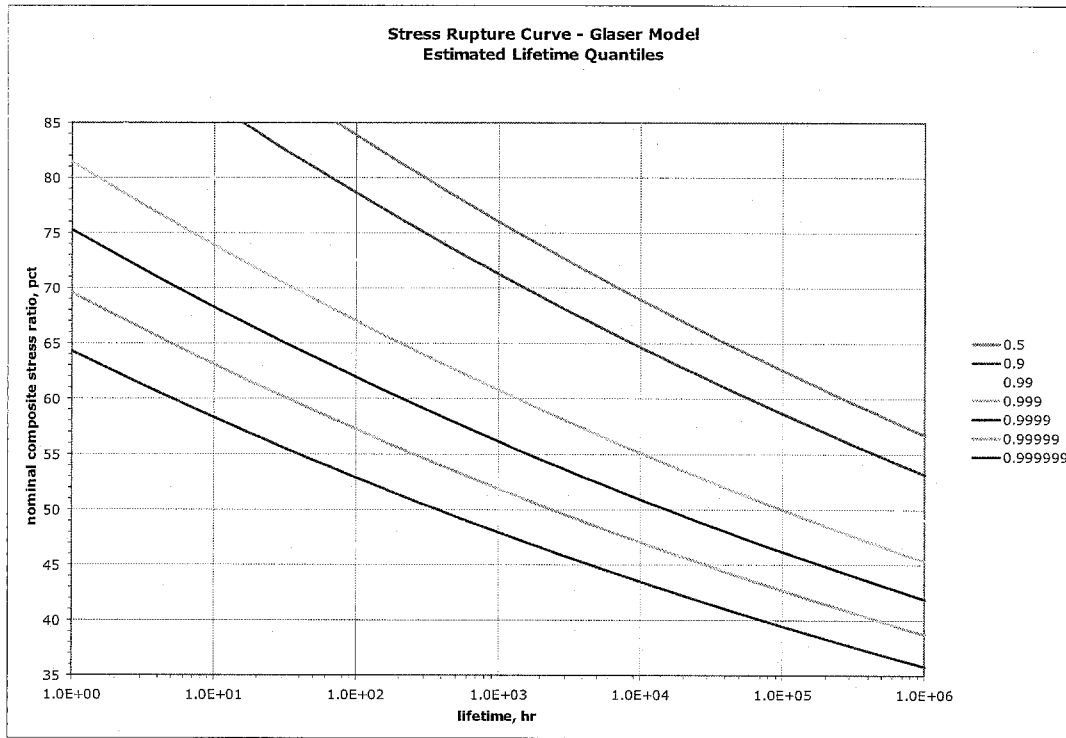


Figure 3. Glaser Stress Rupture Curve. Quantiles are for probability of survival.

### Comparison of Reliability Models from Glaser and Phoenix

Both the Phoenix and Glaser models are based on a power-law framework within the Weibull distribution. This methodology has a basis in early composites failure theory developed by Coleman.<sup>18</sup> The models provide virtually indistinguishable reliability estimates for the Orbiter COPVs, especially when conditional reliability is used. A comparison between results for each model is shown in table 3.

Table 3. Comparison of Reliability Estimates for Using Phoenix and Glaser Models. Estimates are calculated for the next scheduled flight.

Vessel Type	Stress Ratio for Phoenix Model	Stress Ratio for Glaser Model	Past Accumulated Hours	Hours for One Future Mission	No. of Vessels	Non-Conditional		Conditional	
						Phoenix	Glaser	Phoenix	Glaser
OMS	0.575	0.604	4151	252	1	0.994571361	0.995182204	0.99960116	0.99899579
OMS	0.575	0.604	3983	252	1	0.994833253	0.99542157	0.99960434	0.99899579
RCS	0.515	0.541	7551	630	2	0.999066453	0.999187175	0.99990573	0.99962693
RCS	0.515	0.541	6620	395	2	0.999202759	0.999309176	0.99994256	0.99976608
RCS	0.515	0.541	6112	249	2	0.999275571	0.999374093	0.99996443	0.99985253
MPS he	0.54	0.576	858	24	3	0.999596528	0.999483792	0.99998642	0.99990638
MPS He	0.47	0.494	858	24	7	0.999982728	0.999986366	0.99999942	0.99999418
ECLSS N2-1	0.445	0.468	74495	648	1	0.999891619	0.999899715	0.99999887	0.99999373
ECLSS N2-2	0.445	0.468	74495	648	1	0.999891619	0.999899715	0.99999887	0.99999373
ECLSS N2-3	0.445	0.468	74408	648	1	0.999891771	0.999899859	0.99999887	0.99999373
ECLSS N2-4	0.445	0.468	65910	648	1	0.999906428	0.999913803	0.99999889	0.99999373
ECLSS N2-5	0.445	0.468	61793	648	1	0.999913397	0.999920409	0.99999891	0.99999373
ECLSS N2-6	0.445	0.468	22548	648	1	0.999974169	0.999977116	0.99999911	0.99999373
<b>Reliability for Entire System of COPVs=</b>						<b>0.986066333</b>	<b>0.987510562</b>	<b>0.99899791</b>	<b>0.99710314</b>

Table 3 shows the probability of survival estimates using the basic models (non-conditional) and conditional reliability models. For each of the vessel types, the reliability is determined as a function of the number of vessels in that type, so it's the single vessel reliability to the number of vessels of that type. To determine the overall system level reliability, the reliabilities of each vessel type are multiplied to arrive at a reliability estimate for the Orbiter system of COPVs. This similarity of the results despite their independent development lends credibility to both models.

A more general comparison of the basic models is observed in stress rupture curve comparisons. Figure 4 shows a stress rupture curve for the 0.999 and 0.99999 quantile. To calculate values for the curves, equations 2 and 5 were arranged to calculate stress ratios for these quantiles. To establish a fair comparison and eliminate confusion, stress ratios for the Glaser model were modified by 5% to compensate for differing methods of accounting for pressurization rate. The rate difference is built into the Phoenix model, whereas the pressurization rate must be applied to the Orbiter vessels before using the Glaser model. When these differing pressurization rate assumptions are accounted for, the differences in reliability estimates are very small; less than 1%.

To understand why the models provide results that are so similar requires an understanding of differences and similarities of the parameters used. Clearly equations 2 and 4 are similar and the simplification of equation 4 to equation 5 reveals the power-law structure of the Glaser model. To facilitate a comparison, the Glaser model is mapped onto the Phoenix model.

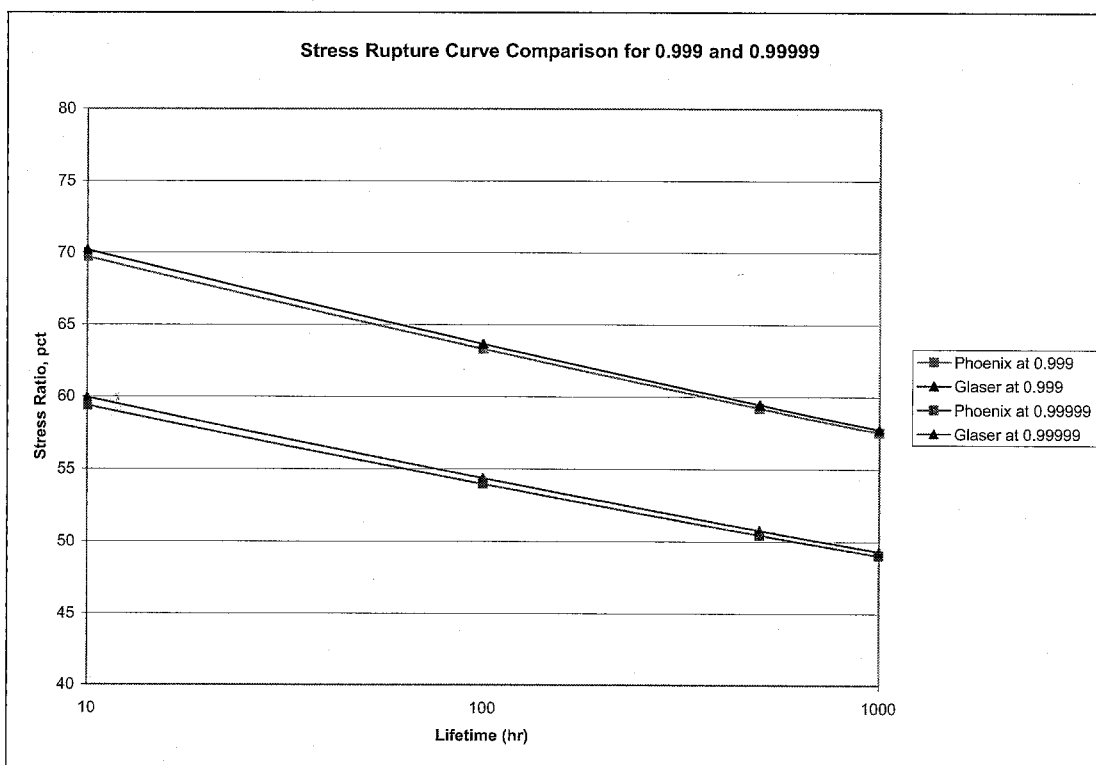


Figure 4. Stress Rupture curve comparison for probabilities of survival of 0.999 and 0.99999.

Rearranging the Glaser model (equation 5), we arrive at equation 7.

$$P\{T_s > t\} = \exp\left[-\left(\frac{t}{e^{\beta_1}} s^{-\beta_2}\right)^{1/\beta_3}\right] \quad (7)$$

Immediate parallels can be drawn between this form and equation 2:  $1/\beta_3$  must be equal to  $\beta$  and  $-\beta_2$  must be equal to  $\rho$ . A comparison of tables 1 and 2 reveal that this is true as summarized in table 4. However, parallels between the Glaser model and the Phoenix parameter of  $t_{c,ref}$  are more difficult. Accounting for differences between the definition of stress ratio by adding a factor,  $r$ , and determining the value of  $e^{\beta_1}$  allows this comparison as illustrated in equation 8.

$$P\{T_s > t\} = \exp\left[-\left(\frac{t}{e^{\beta_1} r^{\beta_2}} s^{-\beta_2}\right)^{1/\beta_3}\right] \quad (8)$$

In equation 8,  $r = \left(\frac{100}{0.95}\right)$ . This factor is needed because the Phoenix model accounts for a 5% pressurization rate effect in the LLNL data and the Glaser model defines stress ratio in terms of percentage of actual burst strength of LLNL vessels, as discussed previously. Calculating a value for  $e^{\beta_1} \cdot r$  from coefficients listed in table 2, a value very similar to  $t_{c,ref}$  is found as seen in table 4.

**Table 4. Parameter and Coefficient comparisons.**

Shape Parameter	$\beta$	1.2
	$1/\beta_3$	1.236
Power Law Exponent	$\rho$	24
	$-\beta_2$	23.602
Time reference	$t_{c,ref}$	0.5456
	$e^{\beta_1} \cdot r$	0.6275

The similarity of these models as evidenced by the similarities between parameter values is surprising since the models were derived using different approaches and the Glaser model had more adjustable parameters that might have provided a better and different fit to the LLNL data and thus, different predictions. These similarities in the behavior of the models lend credibility to both and to the reliability estimations for the Orbiter COPVs. Other models for stress rupture exist and will be explored in future publications.

### Confidence Intervals and Stress Rupture Parameter Sensitivities

The conditional probability of survival is a function of several variables and parameters which have been determined based on limited amounts of data. However, uncertainties do exist, and treating various parameters as deterministic variables and arriving at a single point probability of survival estimate number is hidden with dangers. In order to be able to account for the inherent uncertainties, one should consider the probabilistic aspects of the phenomenon in a more rigorous manner. Accordingly the point probability estimate becomes a random variable and hence one needs to bound this with either upper and

lower confidence bounds or one sided confidence bounds. An attempt is made to capture these in the Phoenix and Glaser models and a comparison of the various methodologies is presented in this section.

Equation 9 is an expression for probability of survival in a generic form as a function of several pertinent random variables

$$P_S(\sigma, t) = F(\sigma_r, t_r, \Delta t_r, \rho, \beta) \quad (9)$$

where

$$\sigma_r = \frac{\sigma_1}{\sigma_{c,ref}}, \quad (10)$$

$$t_r = \frac{t_1}{t_{c,ref}}, \quad (11)$$

$$\Delta t_r = \frac{\Delta t_1}{t_{c,ref}} \quad (12)$$

The symbols  $\rho$ , and  $\beta$  are the power law coefficient and the shape factor respectively. A limit state function (sometimes referred to as performance function) is defined as:

$$g(\bar{X}) = P_S(\bar{X}) - P_{S0} \quad (13)$$

where  $P_{S0}$  is a particular value of  $P_S$ . The vector  $\bar{X}$  represents the various uncertain variables considered in the current problem. The limit state function can be an implicit or explicit function of random variables and is divided in such a way that  $g(\bar{X}) = 0$  is a boundary between the region  $[g \leq 0]$ , which means that a certain level of reliability is not met and  $[g > 0]$ , which means the reliability is met meeting or exceeded. It should be noted that since the cumulative distribution function (CDF) of  $P_S$  at  $P_{S0}$  equals the probability that  $[g \leq 0]$ , the CDF can be computed by varying  $P_{S0}$  and computing the point probability.

The probability that  $[g \leq 0]$ , is given by the integral

$$P[g \leq 0] = \int_{\Omega} \dots \int f_X(X_1, X_2, \dots, X_n) dX_1 dX_2 \dots dX_n \quad (14)$$

in which  $f_X(X_1, X_2, \dots, X_n)$  is the joint probability density function for variables  $X_1, X_2 \dots X_n$  and the integration is performed over the region,  $\Omega$ , where  $g \leq 0$ . If the random variables are statistically independent, then the joint probability density function can be replaced by individual density functions. This integral can be computed by standard Monte Carlo procedure which is rather straightforward. However, depending upon the number of random variables involved and the level of  $P_{S0}$  sought, this must be repeated thousands of times, to accurately build the response variable's probabilistic characteristics. Although inherently simple, the large number of output sets that must be generated to build the CDF of the output variable, becomes its obvious disadvantage. Furthermore, if the deterministic computation of

the response is complicated, time-consuming analysis (e.g. a large non-linear finite element analysis), the time required and the computational costs could become prohibitive.

In our present case, however, we have a closed form expression for the conditional probability for mission survival as given below<sup>19,20,21</sup>

$$P_S(t|\sigma_S^*, t_1) = \frac{\exp \left\{ - \left[ \left( \frac{t_1}{t_{c,ref}} \right) \left( \frac{\sigma_{op1}}{\sigma_{c,ref}} \right)^\rho + \left( \frac{\Delta t}{t_{c,ref}} \right) \left( \frac{\sigma_{op2}}{\sigma_{c,ref}} \right)^\rho \right]^\beta \right\}}{\exp \left\{ - \left[ \left( \frac{t_1}{t_{c,ref}} \right) \left( \frac{\sigma_{op1}}{\sigma_{c,ref}} \right)^\rho \right]^\beta \right\}} \quad (15)$$

Equation 15 is an un-simplified version of equation 3 and is solved using 1,000,000 Monte-Carlo simulations for each class of vehicle. These simulations were performed using the Southwest Research Institute developed code NESSUS ver. 8.2. Details of the theory are outlined in reference 22. The variables considered in the process are listed in Table 5. The survival probabilities for one sided 95% confidence limit are computed for each of the vessels and the results are tabulated in Table 6.

It should be noted that in the above calculations the four random variables are considered to be independent and therefore the resulting confidence limits will be pessimistically wider than the reality. One obvious dependency, for instance, is that since  $t_{c,ref}$  corresponds to a stress ratio of unity, whereas the stress ratio of interest is 0.575, and the data LLNL data itself spans the stress ratio 0.75 approximately, then an estimate on the low side for  $\rho$  will tend to be accompanied by a high estimate for  $t_{c,ref}$  due to the pivot effect around 0.75 stress ratio and this will tend to compensate most of the effect of a low  $\rho$  value. The limits therefore can be considered to be on the conservative side. The correlation between the four variables must be taken in to account if more representative confidence limits are to be sought.

**Table 5. Input random variables and their values chosen for the current illustration.**

Random Variable	Distribution Type	Mean	Coef. Of Variation
$\sigma_{MOP}/\sigma_p$	Weibull	0.575	3%
$\rho$	Log Normal	24	5%
$\beta$	Log Normal	1.2	16%
$t_p$	Log Normal	.5457	5%

**Table 6. Survival probabilities based on 1,000,000 Monte Carlo simulations**

Vehicle Class	Probability of Survival 95% C.L	Probability of Failure 95% C.L.
OMS-He	0.99895211	0.00104789
RCS-He	0.9998385	0.0001615
MPS-B-He	0.99994075	5.925E-05
MPS-S-He	0.99999726	2.74E-06
ECLSS-N2	0.9999805	1.95E-05

Furthermore, the coefficients of variation in the random variables considered are based on current best judgment. A reduction in the variance will give tighter confidence bounds.

A limited study of the deterministic sensitivity of the conditional probability of survival to various parameters of interest was also done and is reported in figure 5. Each variable is normalized with respect to the mean value and is varied one at a time between 0.4 to 1.4. From figure 6, it is clear that the conditional survival probability is most sensitive to variables stress ratio and the power law coefficient  $\rho$ , while it is fairly insensitive to the values of  $t_{c,ref}$  and  $\beta$ .

The results of confidence bounds estimations using various formulations is given along with the point probability of survival estimates in Table 7. Figure 6 shows a pictorial comparison of the probability of failure for each sub-system. In arriving at these results, the past effective times at pressure in hours for each COPV sub-system, as well as the current mission duration hours were best estimates at the time these results were computed. The past times for each of the 24 vessels were independently estimated and the highest number of hours for each COPV sub-system was considered in the calculations to be on conservative side. Since this study was done, based upon the NESC input, several operational as well as other changes were brought in order to minimize the times spent with the view to maximize the reliability and life. As a result the most recent estimations for the hours differ slightly from those reported here. For the purpose of comparison of various models, however, these differences do not affect the qualitative conclusions of the study. Note that although the methodologies used for conditional probability are different in the Glaser and the Phoenix models, the predictions for point probability estimates as well as confidence limit estimates are virtually indistinguishable.

In addition to the present work, extensive discussion and analysis of confidence intervals has been undertaken by the NESC COPV team including Ron Glaser and Leigh Phoenix. It is unclear how confidence intervals can provide additional assurances of the future flightworthiness of the Orbiter COPVs. Discussion of findings and analyses of confidence interval approaches will be provided in future publications, but the results from the confidence interval determination developed by Glaser are shown in figure 6 for comparison with the present analysis.

**Table 7. A comparison of the two methodology predictions**

<b>OV-103 COPV Sub- System</b>	<b>Conditional Probability of Survival/ Phoenix</b>	<b>Conditional Probability of Survival/ Ron Glaser</b>	<b>Phoenix- 95%</b>	<b>Glaser- 95%</b>
<b>OMS He</b>	<b>0.99984546</b>	<b>0.99985216</b>	<b>0.99895211</b>	<b>0.99872706</b>
<b>RCS He</b>	<b>0.99998602</b>	<b>0.99998753</b>	<b>0.9998385</b>	<b>0.99986917</b>
<b>MPS he</b>	<b>0.9999955</b>	<b>0.99999406</b>	<b>0.99994075</b>	<b>0.99993648</b>
<b>MPS He</b>	<b>0.9999992</b>	<b>0.9999993</b>	<b>0.99999726</b>	<b>0.99999887</b>
<b>ECLSS N2</b>	<b>0.99999887</b>	<b>0.99999892</b>	<b>0.9999805</b>	<b>0.99998654</b>

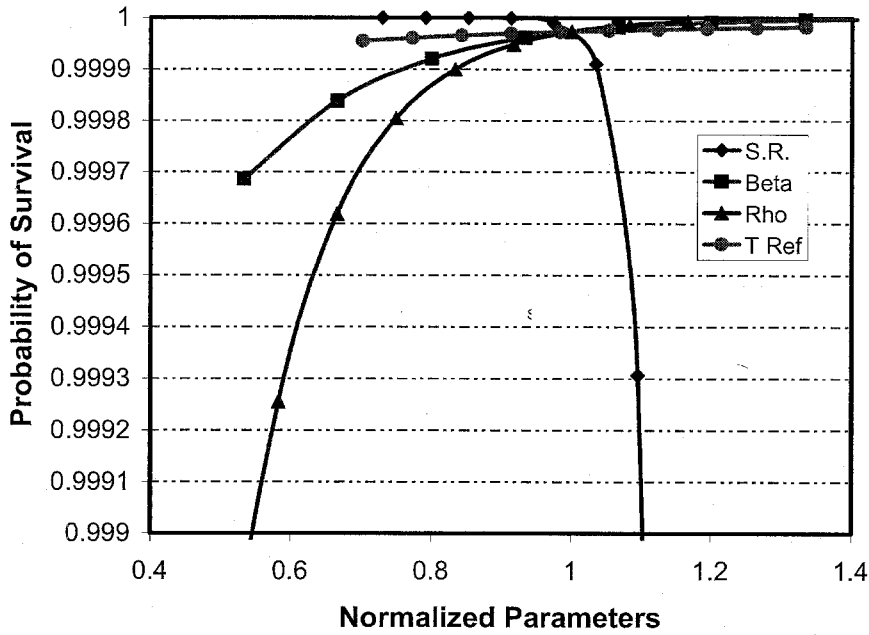


Figure 5. Sensitivity of the conditional probability of survival to various normalized stress rupture life estimation parameters.

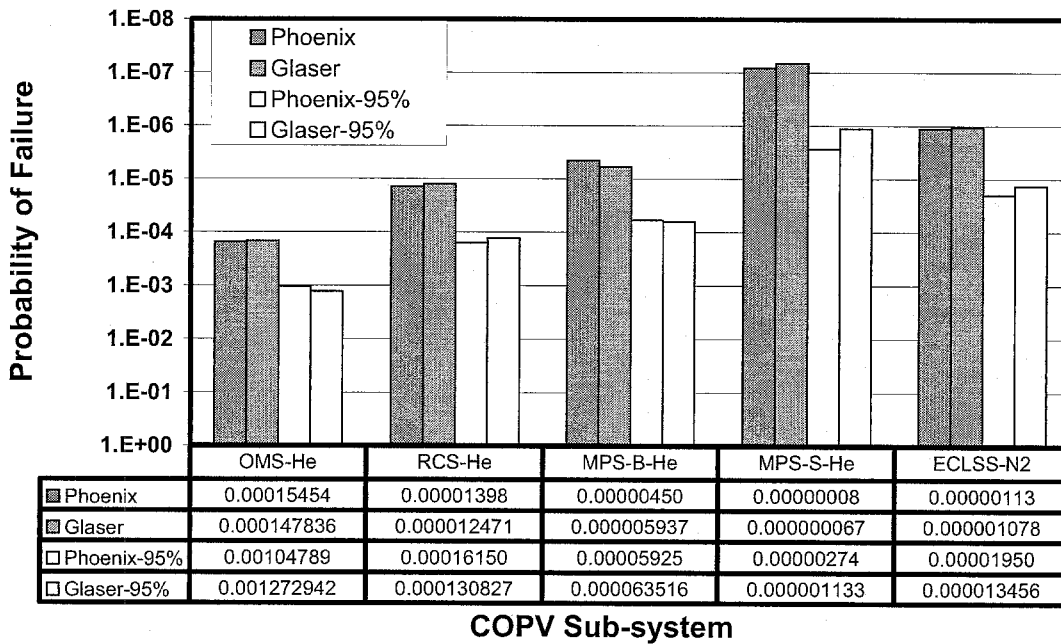


Figure 6. A comparison of all the three methodologies; point and 95% one sided confidence estimates for probability of failure for various COPV sub-systems.

## Conclusion

To provide an assessment to justify continued use of the 24 composite overwrapped pressure vessels on board the Orbiter, stress rupture reliability estimates were provided by Phoenix and Glaser. These estimates are very similar despite differing approaches and this lends credibility to both models which were developed independently. Work is ongoing to understand uncertainty and the role of confidence intervals for future flights of the Orbiter. While work to revise current reliability point estimates is also ongoing, estimates available currently are low based on the Phoenix and Glaser models. Rationale for continued flight will be contingent upon further revision and mitigating actions.

## Glossary of Symbols:

$\sigma_{burst}$	Stress in fiber at burst pressure
$\sigma_{op}$	Stress in fiber at operating pressure
$\sigma_{op1}, \sigma_{op2}$	Stress in fiber at past/present operating pressures
$\sigma_{ref}$	Stress at reference time in the plateau region
$\rho$	Power law coefficient for stress in Phoenix model
$\beta$	Shape parameter
$\beta_1, \beta_2, \beta_3$	Coefficients based on maximum likelihood estimates in Glaser Model
$t$	Time
$t_1$	Past effective time in hours
$t_{c,ref}$	Reference time at the plateau region
$\alpha$	Scale parameter
$P$	Probability
$\Delta t$	Current mission time spent at operating stress ratio
$s$	Stress ratio used in the Glaser model
$r$	Correction factor to account for pressurization rate differences
$g(\underline{X})$	Limit state function
$\underline{X}$	Vector of uncertain variables
$f_x$	Joint probability density function
$\Omega$	Region of uncertain variables

## References

1. NESC Composite Overwrapped Pressure Vessel Independent Technical Assessment Final Report.
2. Glaser, R.E., R.L. Moore, and T.T. Chiao. "Life Estimation of an S-Glass/Epoxy Composite under Tensile Loading." *Composites Technical Review*, Vol. 5, No. 1 (1983): 21-26.
3. Glaser, R.E., R.L. Moore, and T.T. Chiao. "Life Estimation of Aramid/Epoxy Composites under Sustained Tension." *Composites Technical Review*, Vol. 26 (1984): 26.
4. Phoenix, S. Leigh, and E.M. Wu. "Statistics for The Time Dependent Failure of Kevlar-49/Epoxy Composites: Micromechanical Modeling and Data Interpretation." IUTAM Symposium on Mechanics of Composite Materials, Pergamon (1983):135.
5. Thomas, Donald. "Long-Life Assessment of Graphite/Epoxy Materials for Space Station Freedom Pressure Vessels." *Jet Propulsion*, Vol. 8, No. 1 (1992): 87.
6. Wagner, H.D., P. Schwartz, and S. Leigh Phoenix, "Lifetime Statistics for single Kevlar 49 filaments in creep-rupture." *J. Mat. Sci.*, Vol. 21 (1986):1868.
7. Wagner, H.D., S. Leigh Phoenix, and P. Schwartz. "A Study of Statistical Variability in the Strength of Single Aramid Filaments." *J. Comp. Mat'ls*, Vol. 18 (July 1984): 312.
8. Michalske, T.A., and B. Bunker. "A Chemical Kinetics Model for Glass Fracture." *Journal of American Ceramics Society*, Vol. 76, No. 10, (1993): 2613-18.

9. Phoenix, S. Leigh. "Statistical Modeling of the Time and Temperature Dependent Failure of Fibrous Composites." Proceedings of the 9th US National Congress of Applied Mechanics, Book # H00228, ASME, NY (1982): 219-229.
10. Christensen, R., "Interactive Mechanical and Chemical Degradation in Organic Materials", Int. J. Solids Structures, v. 20, No. 8, (1984)791.
11. Phoenix, S. Leigh, and I.J. Beyerlein. "Statistical Strength Theory for Fibrous Composite Materials." *Comprehensive Composite Materials*, Elsevier Science(2000): 1-81.
12. Glaser, R.E., R.L. Moore, and T.T. Chiao. "Life Estimation of Aramid/Epoxy Composites under Sustained Tension." *Composites Technical Review*, Vol. 26 (1984): 26-35.
13. Wagner, H.D., P. Schwartz, and S. Leigh Phoenix, "Lifetime Statistics for single Kevlar 49 filaments in creep-rupture." *J. Mat. Sci.*, Vol. 21 (1986):1868.
14. Glaser, R.E. "Statistical Analysis of Kevlar 49/Epoxy Composite Stress-Rupture Data." LLNL UCID-19849, Sept. 1983.
15. Glaser, R.E., R.L. Moore, and T.T. Chiao. "Life Estimation of Aramid/Epoxy Composites under Sustained Tension." *Composites Technical Review*, Vol. 26 (1984): 26-35.
16. Wu, H.F., S. Leigh Phoenix, and P. Schwartz. "Temperature Dependence of Lifetime Statistics for Single Kevlar 49 Filaments in Creep- Rupture." *Journal of Material Science*, Vol. 23 (1988):1851-1860.
17. Ibnabdeljalil, M., and S. Leigh Phoenix. "Creep Rupture of Brittle Matrix Composites Reinforced with Time Dependent Fibers: Scalings and Monte CARlon Simulations." *Journal of Mechanical Physical Solids*, Vol. 43, No. 6 (1995): 897-931.
18. Coleman, B., "Statistics and Time Dependent Mechanical Breakdown in Fibers", *J. Applied Physics*, v. 29, n. 6, 1958.
19. Methodology for determining reliability of Kevlar COPVs in future missions under reduced operating pressures, S. L. Phoenix, draft 4, April 10, 2005.
20. Update on Reliability Predictions from LLNL Kevlar COPVs (Including Effect of Vessel #188) and Confidence Interval Issues, S. L. Phoenix, June 13, 2005
21. Effect of Uncertainty in our Reliability Calculations, S.L. Phoenix, April 22, 2005
22. FPI User's and Theoretical Manuals, Southwest Research Institute, 1995.

A portion of the research described in this (publication or paper) was carried out at the Jet Propulsion Laboratory, California Institute of Technology, under a contract with the National Aeronautics and Space Administration.